CONTROLLING BROMATE FORMATION BY CONVENTIONAL AND INNOVATIVE TITANIUM DIOXIDE PHOTOCATALYSIS

by

Ryan Brookman

Submitted in partial fulfilment of the requirements
for the degree of Master of Applied Science

at

Dalhousie University
Halifax, Nova Scotia
August 2010

DALHOUSIE UNIVERSITY

DEPARTMENT OF ENVIRONMENTAL ENGINEERING

The undersigned hereby certify that they have read and recommend to the Faculty of Graduate Studies for acceptance a thesis entitled "CONTROLLING BROMATE FORMATION BY CONVENTIONAL AND INNOVATIVE TITANIUM DIOXIDE PHOTOCATALYSIS" by Ryan Brookman in partial fulfilment of the requirements for the degree of Master of Applied Science.

Dated: August 24, 2010

Supervisor: _____
Graham A. Gagnon

Readers: _____
Jeff Dahn

_____
Jennie Rand

DALHOUSIE UNIVERSITY

DATE: August 24, 2010

AUTHOR: Ryan Brookman

TITLE: CONTROLLING BROMATE FORMATION BY CONVENTIONAL AND INNOVATIVE TITANIUM DIOXIDE PHOTOCATALYSIS

DEPARTMENT OR SCHOOL: Department of Environmental Engineering

DEGREE: MASc CONVOCATION: October YEAR: 2010

Permission is herewith granted to Dalhousie University to circulate and to have copied for non-commercial purposes, at its discretion, the above title upon the request of individuals or institutions.

_____

Signature of Author

Dedication Page

To my family, who have always encouraged and supported the pursuit of my next accomplishment.

Table of Contents

List of Tables

List of Figures

Abstract

Titanium dioxide (TiO_2) nanoparticles have disinfection capabilities, but removing them from suspension is not practical for water treatment. The objective of this thesis is to integrate proven ultraviolet (UV) disinfection technology with immobilized TiO_2 supported on nanostructured thin film (NSTF) developed by 3M Company to develop a robust water treatment technology that disinfects without forming regulated disinfection byproducts (DBP), such as bromate and bromoform. Drinking water, artificial brackish water, and seawater were first used to develop a method to detect bromate because the presence of chloride in brackish and seawater complicates bromate detection by ion chromatography. Next, the same three water matrices were monitored for the production of bromate by bench scale UV-TiO_2 and ozone treatments. To compare the effect of UV irradiation on suspended TiO_2 and TiO_2 supported on NSTF, physical and chemical changes of the TiO_2 were monitored by scanning electron microscopy (SEM), and x-ray photoelectron spectroscopy (XPS), respectively. Potential of UV-NSTF for photocatalysis was evaluated by degradation of *para*-chlorobenzoic acid (pCBA), a hydroxyl radical (•OH) probe compound analyzed by high performance liquid chromatography (HPLC). Key findings include a simple and accurate spectrophotometric method for the detection of bromate in saline water. Also, disinfection by UV-TiO_2 did not form bromate at detectable concentrations ($<5\ \mu gL^{-1}$) in any of the water matrices studied, but ozone produced up to $4.5\ mgL^{-1}$ of bromate. Additionally, bromoform and DBP precursors were consistently lower in UV-TiO_2 experiments than in ozonation trials. Lastly, TiO_2-NSTF was found to produce •OH on the same order of magnitude as suspended TiO_2 nanoparticles (10^{-15} molar). Overall, this thesis portrays the potential of innovative TiO_2 nanomaterials in photocatalytic oxidation as a future disinfection method in various water treatment applications.

List of Abbreviations Used

AOP	advanced oxidation process
Br^-	bromide
Br_2	total bromine
BrO_3^-	bromate
$CHBr_3$	bromoform
DBP	disinfectant/disinfection byproduct
DO	dissolved oxygen
DOC	dissolved organic carbon
eV	electron volts
GC/MS	gas chromatography coupled with mass spectrometry
H_2O_2	hydrogen peroxide
HAA	haloacetic acid(s)
HOBr	hypobromous acid
HPLC	high performance liquid chromatography
I	iodide
IC	ion chromatography
ICP/MS	inductive coupled plasma mass spectrometry
IMO	International Maritime Organization
k^*	net rate coefficient
M	molar concentration
MCL	USEPA's maximum contaminant level
MCLG	USEPA's maximum contaminant level goal
MDL	method detection limit
mgL^{-1}	milligram per liter
mJ	millijoule
nm	nanometer
NOM	natural organic matter
NSERC	Natural Science and Engineering Research Council of Canada
NSTF	nanostructured thin film developed and manufactured by 3M Company
$\bullet O_2^-$	superoxide radical(s)

O_3	ozone
OBr^-	hypobromite ion
•OH	hydroxyl radical(s)
ORP	oxidation-reduction potential
pCBA	*para*-chlorobenzoic acid
ppt	parts per thousand
ROS	reactive oxygen species
SEM	scanning electron microscopy
THM	trihalomethane(s)
TiO_2	titanium dioxide
TOC	total organic carbon
μgL^{-1}	microgram per liter
µm	micrometer
μScm^{-1}	microsiemens per centimeter
USEPA	United States Environmental Protection Agency
UV	ultraviolet light
XPS	x-ray photoelectron spectroscopy

Acknowledgements

This work was funded by the Natural Science and Engineering Research Council of Canada (NSERC) through the NSERC/Halifax Water Industrial Research Chair program.

Trojan Technologies loaned the collimated beam to the Aquatron laboratory at Dalhousie University. 3M Company provided the nanostructured thin film to the Physics Department at Dalhousie University.

Thank you to John Batt and Jim Eddington at Dalhousie's Aquatron, Dr. Zeynel Bayindir, Dr. Robbie Sanderson, and Pat Scallion in Dalhousie's Institute of Research in Materials. Also, the help of Dr. Robbie Sanderson in Dalhousie's Department of Physics and Atmospheric Science, and Pat Scallion in Dalhousie's Institute of Research and Materials is recognized and appreciated. Janeen McGuigan and Amy McClintock in the Water Quality Laboratory at Dalhousie University were very helpful. Most of all, thank you to Heather Daurie, Dalhousie University's Water Quality Laboratory Technician, for all of her patient guidance and expertise.

The time and interest invested by Dr. Jeff Dahn and Dr. Jennie Rand to attend committee meetings, review this thesis, and offer valuable advice and support is greatly appreciated. Dr. Graham Gagnon has been extremely instrumental in directing the course of this research. His keen supervision and enthusiastic encouragement have played important roles in making the construction of this thesis enjoyable.

Chapter 1 Introduction

1.1 Background

1.1.1 The Use of Advanced Oxidation Processes in Water Treatment

Drinking water treatment systems aim to provide safe water for their communities. An important aspect to the treatment process is the removal or inactivation of organisms that could be harmful. The most common disinfection method involves adding chlorine to kill bacteria, viruses, and other microorganisms. While chlorine is very effective, the reactions that occur with natural organic matter (NOM) present in all source waters have the potential to produce various disinfectant/disinfection byproducts (DBP), which are known to cause birth defects and be carcinogenic (Singer, 2006). To reduce the formation of DBPs, other disinfection steps called advanced oxidation processes (AOPs) have been investigated. AOPs (i.e., ozone and UV-based technologies) generate highly reactive oxygen species (ROS), most notably the hydroxyl radical (•OH). Matilainen and Sillanpaa (2010) stated "the appeal of AOPs is the possibility to gain complete oxidation or mineralization of organic contaminants through a process that operates near ambient temperature and pressure." Despite favorable results, the use of AOPs is still very limited in full-scale applications due to several resource constraints such as cost and experienced operators. However, AOPs are among the most studied technologies for purification and disinfection of water (Matilainen and Sillanpaa, 2010).

The basis of disinfection by AOPs is their ability to produce hydroxyl radicals (•OH). These radicals are highly non-specific, and very strong oxidants (Elovitz and von Gunten, 1999). In water, they are produced by the decomposition of ozone (O_3), and by the photoactivation of compounds such as hydrogen peroxide (H_2O_2) and titanium dioxide (TiO_2). The production of •OH is what makes AOPs lucrative to the water industry. Cho et al., (2008) reported the oxidation potential of •OH was greater than ozone, chlorine dioxide, and free chlorine. Thus, inactivation of *Cryptosporidium parvum* was more easily achieved by •OH than other disinfection methods. The strong oxidation power of •OH can disinfect a variety of microorganisms, as well as mineralize environmental contaminants (Hand et al., 1995). AOPs offer the production of •OH as well as increased disinfection efficiency and decreased NOM. However, not all AOPs provide the same

quality of treatment. For example, some processes are better at NOM reduction than disinfection of certain organisms. Matilainen and Sillanpaa (2010) stressed that knowing the treatment objective is highly important when selecting the proper advanced oxidation technology.

1.1.2 Types of Advanced Oxidation Processes

The water industry currently employs AOPs in both drinking water and wastewater applications. The most common AOPs are UV-based and ozone-based technologies. Research into combining UV and O_3 with other compounds to increase •OH production is readily available. Among the compounds being investigated for combination with UV-based technologies are H_2O_2 (Rosenfeldt and Linden, 2007; Song et al., 2004; Watts et al., 2007) and suspended TiO_2 nanoparticles, called photocatalysis (Brunet et al., 2009; Cho et al., 2005; Gerrity et al., 2008; Tercero Espinoza and Frimmel, 2008).

Ozone disinfection is a two-pronged mechanism and has long been used for disinfection, taste and odor management, as well as color removal in water treatment (Matilainen and Sillanpaa, 2010; von Gunten, 2003a). Molecular O_3 is a strong oxidant, but as it dissociates in water, •OH, even stronger oxidants, are produced. Elovitz and von Gunten (1999) reported that 10 μM ozone formed a steady state •OH concentration on the order of 10^{-13} M, typical for ozonation of Swiss waters. In addition to •OH production efficiency, ozonation leaves a measurable residual in the distribution system when used for drinking water. The drawbacks of disinfection by O_3 include DBP formation and energy required to produce O_3 from compressed oxygen. Singer (2006) considered brominated DBPs, including bromate and bromoform to be more dangerous than their chlorinated counterparts (i.e., trihalomethanes and haloacetic acids, or THMs and HAAs, respectively). This is a severe disadvantage for ozonation, as the formation of brominated DBPs is not only prevalent, but also hard to mitigate in waters that contain bromide. Drinking water sources can contain bromide from many possible sources such as seawater intrusion in coastal areas, industrial effluents or geological formations upstream. Applications of ozone outside the drinking water industry mainly deal with saline systems where bromide is abundant. Tango and Gagnon (2003) reported that the

use of O_3 in marine aquaculture systems forms bromate that negatively impacts the health of the fish, and Jones et al. (2006) reported the toxicity levels of brominated DBPs to marine organisms. The formation of dangerous brominated DBPs by ozonation, combined with the energy required to produce O_3 makes it a less than desirable option for ballast water and aquaculture systems.

Disinfection by TiO_2 is primarily accomplished by •OH formation. During the photoactivation of TiO_2 by UV light (wavelength less than 387 nm (Linsebigler et al., 1995)), electrons are excited from the valence band to the conduction band. The result is an electron-hole pair, in which the electron reduces oxygen in the water to form superoxide radicals that either oxidize organic species, form H_2O_2 radicals and •OH, or eventually become water again (Linsebigler et al., 1995). The photogenerated hole is capable of directly oxidizing molecules that are adsorbed on the surface, as well as reacting with hydroxyl groups on the surface to form •OH (Linsebigler et al., 1995). The result of the photoactivated TiO_2 is the production of highly reactive radical species (Brunet et al., 2009). However, in photocatalysis of TiO_2, the TiO_2 particles themselves are the limiting factor. Suspended TiO_2 nanoparticles are capable of producing •OH, but as the concentration of suspended particles increase, the water becomes more turbid and fewer particles are excited. Additionally, as concentration of TiO_2 increases, more microorganisms are shielded from exposure to UV light, resulting in lower inactivation (Gerrity et al., 2008; Matilainen and Sillanpaa, 2010). While suspended TiO_2 reactors have been used in a few wastewater systems, the suspended particles require removal after photocatalysis; this step is complex and costly, thus commercially prohibitive (Thiruvenkatachari et al., 2008). Despite these drawbacks, UV-TiO_2 continues to be studied as an AOP for water treatments systems, including ballast water (Gregg et al., 2009).

1.1.3 UV-TiO_2 Photocatalysis

The potential of UV-TiO_2 photocatalysis as an AOP is based on three aspects of the technology: known effectiveness, synergy and ease of integration with UV systems, and potential TiO_2 immobilization techniques. The effectiveness of UV-TiO_2 treatments on

bacteria (Cho et al., 2004), viruses (Gerrity et al., 2008), and other environmental contaminants (Hand et al., 1995), as well as the reduction of NOM (Matilainen and Sillanpaa, 2010), are well documented. Disinfectant synergy was described by Koivunen and Heinonen-Tanski (2005) as when the "efficiency of combined disinfection method is greater than the efficiency achieved when summing the effects of individual disinfectants." Current UV systems have shown synergistic enhancement when TiO_2 is added to the treatment (Kwon et al., 2008).

To easily and practically integrate TiO_2 into commercial AOPs, various techniques of immobilization of TiO_2 have been presented. TiO_2 immobilization methods include the sol-gel process (Balasubramanian et al., 2003), thin and thick films (Chen and Dionysiou, 2006, 2008), and coating glass beads (Peller et al., 2007). However, none of these methods are currently used for TiO_2 photocatalysis in the water treatment industry. The need for a practical method of immobilizing TiO_2 for easy integration into current UV reactors is clearly still a priority in the development of UV-TiO_2 AOPs. Matilainen and Sillanpaa (2010) stated that the drawback of stabilizing the TiO_2 catalyst leads to reduction in surface area available for reactions compared to suspended particles. Thus, they recommend that immobilization techniques must have very high surface areas in order to be a viable AOP.

1.1.4 Innovative Catalyst Support

Debe and Poirer (1994) presented a unique organic film that was later used as a catalyst support in the fuel cell industry (Debe, 2003). The organic film is comprised of 3 to 5 billion crystalline organic pigment support whiskers per cm^2 that are attached to an advanced polyimide carrier sheet. Each whisker is approximately 1 μm long and 50 nm in diameter (Debe, 2003). The nanostructured thin film (NSTF) developed and manufactured by 3M Company offers the benefit of a high surface area (surface area enhanced by a factor of ~ 10 - 15 cm^2 depending on whisker length and density (Debe, 2003)) that can be coated with any desired material, including TiO_2. The NSTF is coated with any desired thickness of TiO_2 by magnetron sputter deposition (Dahn et al., 2002).

The use of NSTF in the water treatment industry to stabilize a photocatalyst (e.g., TiO_2) offers three great advantages. The first advantage is the high surface area of the resulting thin film of TiO_2 that is made available for reaction sites as recommended by Matilainen and Sillanpaa (2010) in order to be a viable AOP. The second advantage is that NSTF is currently being used and manufactured by 3M Company (Debe et al., 2006; Gancs et al., 2008), so the innovative use of a technology being utilized in a different industry would be easier to master than developing the method independently. Lastly, because NSTF is coated with TiO_2 by magnetron sputter deposition, properties of the TiO_2 film can easily be manipulated (Bonakdarpour et al., 2008; Dahn et al., 2002; Liu et al., 2010).

1.1.5 Development of a New Technology

The development of a new treatment technology in which immobilized TiO_2 could be easily integrated with existing UV systems to improve disinfection would be of interest to the water industry. Wastewater treatment plants that currently use suspended TiO_2 slurry reactors would benefit from not having to remove the nanoparticles. The microfiltration or nanofiltration steps required to remove the TiO_2 would be unnecessary, reducing the cost of membrane replacement (fouled by TiO_2 during removal). The uncertainties involved with potentially releasing the nanoparticles into the environment (Auffan et al., 2009; Hartmann et al., 2010) would be less of an issue with NSTF technology, although TiO_2 nanoparticles are generally considered to be environmentally benign (Linsebigler et al., 1995; Matilainen and Sillanpaa, 2010).

The UV technology currently being used in drinking water could be easily modified to take advantage of TiO_2 coated NSTF. Lower energy UV light-emitting diode (LED) lamps being considered for water treatment (Matilainen and Sillanpaa, 2010) could be designed for use with TiO_2-NSTF. The transition from conventional UV treatment to TiO_2 photocatalysis could provide an upgrade to current disinfection levels (Linsebigler et al., 1995). By increasing disinfection efficiency, the resulting energy consumption required per unit of water treated would be reduced (Bottero et al., 2006). Plants that currently utilize O_3 for disinfection could eliminate the risk of DBP formation (i.e., bromate and bromoform) by converting to UV-TiO_2 technology (Bonacquisti, 2006;

Tercero Espinoza and Frimmel, 2008; von Gunten and Hoigne, 1994). The conversion would also result in an energy reduction and therefore a cost-savings to the utility. Desalination plants could also benefit from a practical UV-TiO_2 technology. Pre-treating source water with TiO_2 photocatalysis could reduce NOM, thus extending the life of the reverse osmosis membrane before fouling occurs (Matilainen and Sillanpaa, 2010). This could potentially be a cost-saving step in an already expensive process.

As ballast water management becomes a requirement for the marine shipping industry (International Maritime Organization, 2009), a suitable technology for the treatment of diverse water matrices will be necessary. However, a "catch-22" situation exists: in order for ballast water management to become international law, a feasible technology must be available. Several technologies and systems have been considered (Dobroski et al., 2009; Gregg et al., 2009), but none have become accepted options for the ballast water management industry. The development of an immobilized UV-TiO_2 technology that would be capable of effective disinfection without forming environmentally harmful DBPs combined with having a small footprint would, at least, be considered for ballast water treatment.

1.2 Rationale and Impact

Ultraviolet (UV) technology is a proven treatment technology for municipal drinking water, wastewater and many diverse industrial applications in water treatment. UV lamps have a small footprint, and disinfection with UV does not result in the release of harmful chemicals such as chlorine and ozone by-products into the environment (Malley et al., 1996). UV disinfection performance can be synergistically enhanced when TiO_2 photocatalyst is used in combination with UV treatment. There is also potential for reduced energy consumption and superior disinfection using TiO_2 and UV compared to using UV alone.

UV-TiO_2 disinfection has been widely used in wastewater treatment applications as a suspended slurry reactor; however, this technique requires separation of TiO_2 from water

after the photocatalytic process (Thiruvenkatachari et al., 2008). From a commercial perspective, this represents a significant challenge associated with UV-TiO_2 reactor designs, as the uncertainty in releasing TiO_2 in the environment or recapturing of the catalyst has been a constraint in practical design and application.

Another benefit of UV-TiO_2 disinfection technology is the minimal, or complete lack of, disinfection/disinfectant byproduct (DBP) formation when compared to conventional disinfection steps like chlorination and ozonation. As water treatment standards and regulations become more stringent, technologies that provide the same level of treatment without the undesired DBP formation will be in high demand if these technologies can be both economical and practical.

1.2.1 Current State of Advanced Oxidation Processes

Both UV and O_3 technologies have been applied in the water treatment industry. Wastewater treatment plants have been using open-channel UV systems to treat their effluents, while drinking water systems only utilize closed-channel UV reactors to ensure higher levels of disinfection of target organisms. O_3 is currently used in drinking water treatment as a disinfection step. The use of UV and O_3 technology has also been considered for the treatment of ballast water in the marine shipping industry (Dobroski et al., 2009; Gregg et al., 2009).

1.2.2 New Applications of Advanced Oxidation Processes

By 2016, the International Maritime Organization (2009) will have introduced new international standards requiring all ships to treat ballast water in order to reduce the spread of non-indigenous and invasive species to fragile coastal ecosystems. This will have a significant impact on the operations of approximately 50,000 ships worldwide. Currently, one of the few treatment methods available for ballast water is ozonation. Aside from the byproducts formed, ozone is less than ideal for ballast water treatment because it must be produced on board the ship; ozone production is very fuel intensive and requires the use of valuable cargo space. UV technology has been considered as an

alternative to O_3 to avoid DBP formation, and high energy requirements (Dobroski et al., 2009).

1.2.3 Controlling Micropollutants in Drinking Water

Titanium dioxide nanoparticles have been used in advanced oxidation applications to successfully treat various environmental pollutants in water (Cho et al., 2005; Hand et al., 1995). However, TiO_2 photocatalysis is still highly experimental and has not been widely employed. In comparison, a well understood and widely used chemical oxidant is ozone (O_3), which reacts with bromide ions (Br^-) naturally present in seawater or brackish water to create toxic byproducts such as bromate (BrO_3^-) (von Gunten and Hoigne, 1994). The USEPA (2009) has identified bromate as a contaminant that increases the risk of cancer, and has set a maximum contaminant level (MCL) of 0.010 mgL^{-1} for drinking water, with a goal (MCLG) of reducing this limit to zero. Compliance with the MCLG for bromate is increasingly difficult for water treatment plants where bromide ions are inherent in the source water, or increased sea water intrusion may occur as a result of predicted sea level rise (Bonacquisti, 2006; Butler et al., 2005). This research intends to illustrate that UV-TiO_2 disinfection controls bromate and bromoform formation to levels below detection limits in both brackish and seawater.

1.2.4 New Method to Detect Bromate in Saline Waters

Bromate concentration in water is detected, typically, by ion chromatography. The USEPA (1999) Method 300.1 describes the methodology for measuring bromate in this manner. However, the peaks that indicate the concentration of bromate on the ion chromatograph occur at approximately the same retention time as chloride. This is not an issue for freshwater samples as the chloride concentration is zero, or very low which results only in small peaks next to bromate, thus bromate detection by conventional methods (i.e., ion chromatography) can be used. If the sample contains large amounts of chloride, such as in brackish water or seawater, the large chloride peak has a base wide enough to interfere with, or completely disguise any bromate peak that may be present.

Previous studies (Afkhami et al., 2001; Ensafi and Dehaghi, 2000; Fukushi et al., 2009) have used variations of a spectrophotometric approach to determine bromate concentrations. This research includes an experimental study to develop a method that utilizes the reaction of bromate with iodide at low pH, and the resulting UV absorbance at 352 nm. The method can be applied for bromate concentrations in saline systems in which chloride interferes with detection by traditional analytical methods. The method will be presented to the Akron Zoo for use in their aquarium systems.

1.2.5 Innovative Materials for UV Technology

Drinking water utilities would be interested in a technology that could provide a cost savings without sacrificing water quality. By using an advanced, polyimide nanostructured thin film (NSTF) developed by 3M Company, and magnetron sputter deposition of TiO_2, the photocatalytic benefits of TiO_2 can be further exploited in the water treatment industry because it is not suspended and does not require removal. Additionally, due to the increased surface area of the NSTF, more TiO_2 can potentially be exposed to less UV light and still achieve the required level of disinfection. The energy saved by using less UV light to accomplish equivalent disinfection translates to a "greener" disinfection step, and potentially a cost savings for the utility. This research integrates immobilized TiO_2 with UV technology to progress towards a low-energy consumption alternative to conventional stand-alone UV systems while decreasing the risk of disinfectant/disinfection byproduct (DBP) formation. In addition, this research investigated the ability of TiO_2 coated NSTF to produce hydroxyl radicals (•OH), which are responsible for the oxidation and disinfection observed during photocatalysis.

1.3 Technical Objectives

The overall objective of the project was to develop an innovative and robust water treatment technology that integrates catalyst nanostructured thin film support with UV disinfection technology (NSTF-UV). Several sub-objectives were studied to achieve this overall goal, as shown below.

i) Develop a method for detecting bromate in saline water.

ii) Compare bromate formation following UV-TiO_2 oxidation to ozonation in salt water. The byproducts monitored were bromate and bromoform.

iii) Illustrate that NSTF-UV is a viable water treatment technology by determining and comparing hydroxyl radical production between photoactivation of nanoparticle TiO_2 and TiO_2 coated NSTF using *para*-chlorobenzoic acid (pCBA). Concurrently, the formation of byproducts continued to be monitored.

iv) Evaluate TiO_2 stability throughout the treatment process. The nanoparticles themselves, as well as the NSTF film were analyzed for physical and chemical changes by scanning electron microscopy (SEM) and x-ray photoelectron spectrometry (XPS).

1.4 Organization of Thesis

This thesis is organized as a "publication format" thesis. A general introductory chapter outlines the rationale and impact of the research. Second, the materials and methods used to obtain and analyze all data are described. The following three chapters discuss the technical objectives previously presented in section 1.3. As this is a "publication format" thesis, these chapters each include an individual abstract, introduction and literature review, materials and methods, results and discussion, and a conclusion specific to that chapter. Additionally, these chapters were written for review and possible publication. The journal to which they have been submitted is stated at the beginning of each chapter. Next, a general conclusion chapter synthesizes the outcomes obtained, discusses how the technical objectives were met, and recommends future work. Finally, references and additional data are provided.

Chapter 2 Materials and Methods

2.1 Sample Preparation

Seawater having a salinity of 30 parts per thousand (ppt) and 44 mgL^{-1} bromide was pumped from the Northwest Arm of Halifax Harbour into the Aquatron at Dalhousie University in Halifax, Nova Scotia, Canada. Artificial brackish water was created by combining raw water from Tatamagouche, Nova Scotia and seawater in a 50:50 ratio, which yielded a salinity of 15 ppt, and 22 mgL^{-1} bromide. The French River is the raw water source for Tatamagouche. For the experiments studied, the French River water samples had a pH of 7.5, alkalinity of 33.1 mgL^{-1} $CaCO_3$, total organic carbon (TOC) concentration of 5.3 mgL^{-1}, and turbidity of 0.1 NTU. The French River does not contain naturally occurring bromide. All water samples were 250 mL and were passed through a 0.45 μm filter prior to disinfection.

2.2 Suspended TiO_2 Irradiation

Degussa P25 anatase titanium (IV) oxide nanopowder (99.7% trace metals basis, Sigma Aldrich, St. Louis, MO) was mixed with Milli-Q water and continuously stirred prior to being spiked into the sample and exposed to UV. Samples were irradiated using a low pressure UV lamp in the collimated beam shown in Figure 1 (Trojan Technologies, London, ON) by following the standardized testing protocol for collimated beam disinfection (Kuo et al., 2003). Fluence values were achieved using a radiometer (International Light Technologies 1400A, Peabody, MA) in accordance with the methods described by Bolton and Linden (2003) which take into account water, divergence, reflection and Petri factors associated with collimated beam experiments.

Figure 1. Collimated beam loaned by Trojan Technologies.

2.3 Ozonation

Samples were ozonated using the corona discharge method in a bench scale semi-batch apparatus depicted in Figure 2. Compressed air was passed into the ozone generator (VMUS-4, AZCO Industries, Ltd., Langley, BC) where high voltage corona discharge causes the breakdown of oxygen molecules into oxygen radicals that combine with the oxygen molecules to form O_3. The produced O_3 is passed into the contactor through tubing. Residual O_3 was collected using a flask that contained potassium iodide solution. O_3 was introduced into the samples by a fine bubble diffuser at a flow rate of 2 $Lmin^{-1}$.

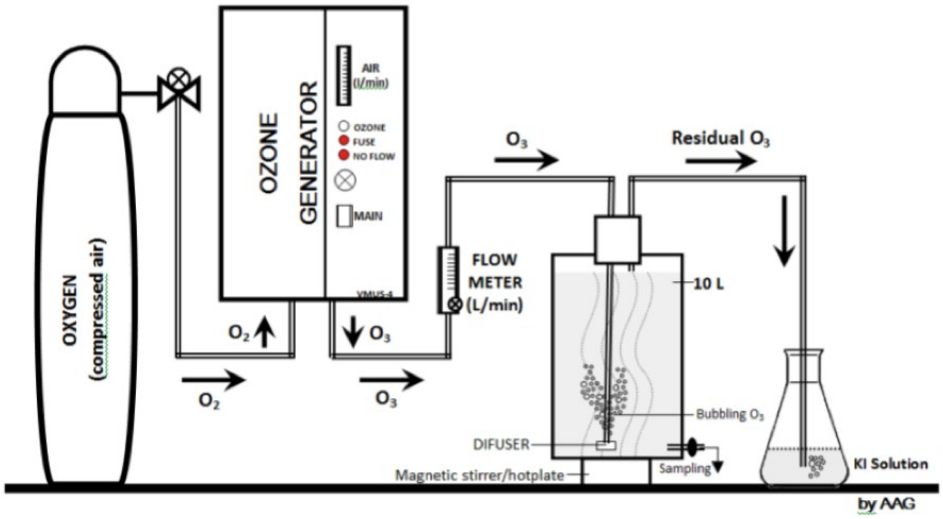

Figure 2. Bench-scale ozonation setup.

2.4 Scanning Electron Microscopy (SEM)

TiO_2 nanoparticles were applied to a carbon tape and prepared for SEM by sputter coating with a Polaron SC7620 using gold/palladium in argon gas with a plasma current of 18 mA for 120 seconds. TiO_2 nanoparticle agglomerates were separated from sample slurries by filtration with 0.45µm filter paper. The filter paper and nanoparticles were then prepared in the same manner. Images were obtained using a Hitachi S-4700 scanning electron microscope.

2.5 X-ray Photoelectron Spectroscopy (XPS)

The samples were analyzed with a Multilab 3000 XPS system manufactured by Thermo VG Scientific. The XPS data were collected with a dual anode x-ray source using Mg Kα61537; irradiation energy of 1253.6 eV. Binding energies are measured using a hemispherical energy analyzer with fixed pass energy of 50 eV that gives an energy resolution of approximately 1.1 eV. The spectra were collected over a sample area of 600 µm in diameter. The C1s peaks were measured and set to 285 eV to account for any charging on the surface of the sample. The data were analyzed using XPS data analysis software, Avantage, version 3.99 developed by Thermo VG Scientific. Fittings of the

peaks are performed using Gaussian-Lorentzian product function and Shirley background algorithm.

2.6 Chemical Methods

Bromine residuals were measured as Br_2 using USEPA Method 8016 to monitor formation of OBr^-, HOBr, and bromamines (Hach DR/2800 spectrophotometer). Other test parameters measured throughout the photocatalysis experiment were pH, dissolved oxygen (DO), salinity and oxidation-reduction potential (ORP) (Fisher Scientific Accumet Excel XL60 meter and corresponding electrodes). Samples were tested prior to being spiked with TiO_2 and again after exposure to UV to determine the byproducts and secondary disinfectants formed during photocatalysis. To measure dissolved organic carbon (DOC), samples were first passed through a 0.45 μm filter, and then preserved by adjusting the pH to less than two with phosphoric acid. The samples were then analyzed according to Standard Method 5310 (for TOC) on Shimadzu TOC VCPH Total Organic Carbon Analyzer. Ozonation of seawater typically forms bromate and bromoform as byproducts. Both ozonated and photocatalysis samples were analyzed for the formation of bromoform by gas chromatography coupled with mass spectrometry (GC/MS) according to USEPA Method 524.2 (2000) and bromate by ion chromatography (IC) according to USEPA Method 300.1 (1999). The method detection limits for bromate and bromoform were 5 μgL^{-1} and 5.9 μgL^{-1}, respectively.

2.7 Analysis of pCBA by HPLC

Para-chlorobenzoic acid (pCBA), shown in Figure 3, is a well known, and commonly used hydroxyl radical probe compound (Brunet et al., 2009; Cho et al., 2004; Cho and Yoon, 2008; Elovitz and von Gunten, 1999; Pi et al., 2005). In this study, pCBA was detected and quantified by high performance liquid chromatography (HPLC). The concentration of pCBA was analyzed by HPLC (Series 200, Perkin Elmer, Milford, MA) according to the method described by Brunet et al., (2009) that employed a Nova-Pak C_{18} reverse-phase column (Waters, Milford, MA, 3.9 mm by 150 mm). The mobile phase was

50% Milli-Q water and 50% acetonitrile. A flow of 0.4 $Lmin^{-1}$ was used along with a UV detector (Series 200, Perkin Elmer, Waltham, MA) at a wavelength of 232 nm to detect the concentration of pCBA. Figure 4 shows how Pi et al., (2005) assumed pCBA reacted with hydroxyl radicals produced by aqueous ozone. pCBA is known to have low reactivity with ozone (Elovitz and von Gunten, 1999; Yao and Haag, 1991) and UV (Pereira et al., 2007), but to react readily with hydroxyl radicals (Elovitz and von Gunten, 1999; Neta and Dorfman, 1968).

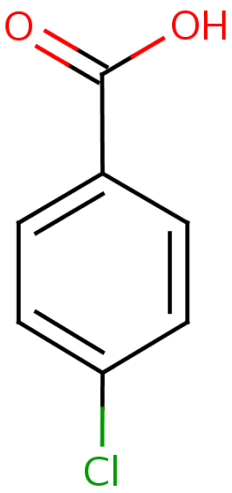

Figure 3. Molecular structure of *para*-chlorobenzoic acid (pCBA).

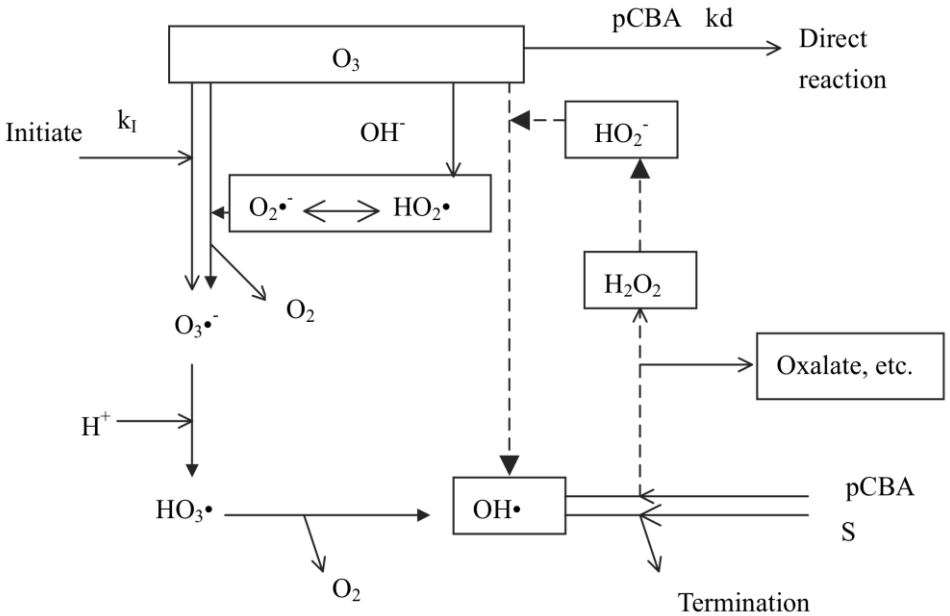

Figure 4. From Pi et al., (2005). An assumed reaction pathway of *para*-chlorobenzoic acid (pCBA) with aqueous ozone.

2.8 TiO_2 on Nanostructured Thin Film (NSTF) Support

Debe et al. (1995; 1994) describes the production and characterization of nanostructured thin film (NSTF) catalyst supports developed by 3M Company (St. Paul, MN) for use in the fuel cell industry. The NSTF consists of 3 to 5 billion crystalline organic pigment support whiskers per cm^2 attached to an advanced polyimide carrier sheet that can be coated with any desired material (Bonakdarpour et al., 2008; Dahn et al., 2002; Debe and Drube, 1995; Debe and Poirier, 1994). For this study, NSTF was coated with titanium dioxide by magnetron sputter deposition as described by Dahn et al. (2002) using two titanium dioxide targets and constant mask openings. The depositions produced catalyst-coated whisker films with a planar loading equivalent of 0.125 mg TiO_2 cm^{-2}.

2.9 Inductively Coupled Plasma Mass Spectrometry (ICP-MS)

Samples that were exposed to TiO_2 coated NSTF were analyzed for any loss of titanium from the NSTF into the water sample. The samples were sent to the QEII Health Science Center in Halifax, Nova Scotia to be analyzed by ICP-MS for trace levels of titanium. The detection limits for titanium were 2 μgL^{-1} in fresh water samples, and 20 μgL^{-1} in saline samples.

2.10 Statistical Analysis

Data were analyzed by the methods described in Berthouex and Brown (1994). Analyses such as the Student *t* test and the F-test were typically performed at the 95% confidence level, unless stated otherwise. Regression analyses were performed using Systat's SigmaPlot 10 software.

Chapter 3 A Method for Detecting Bromate in Saline Water

* A modified version of this Chapter was submitted to *Water Research* in August 2010.
Co-authored by Amy McClintock and Graham Gagnon.
Author provided the major contribution to this manuscript.

3.1 Abstract

The objective of this study was to develop a quick and simple, yet accurate method for the detection of bromate in brackish water. Bromate detection by ion chromatography, the most commonly used method, is complicated by the presence of chloride ions. Both chloride and bromide are present in brackish raw water that may be used for potable purposes. The study was carried out in a laboratory setting using a UV-spectrophotometer and an ion chromatograph to verify the results. To examine the robustness of the UV-based method, seven water matrices were used to test the bromate detection method. The bromate method presented herein utilizes a reaction of bromate with iodide followed by detection at a UV absorbance at 352 nm. A key finding from the study was that the concentration of bromate was quickly and accurately determined using spectrophotometry. This method successfully measured bromate in waters containing a broad range of conductivity and avoided interference from other anions. The method detection limit reported for all seven water matrices tested was greater than 0.14 mgL^{-1}, which limits the method's utility to saline solutions.

KEY WORDS: iodide, bromate, seawater, ozone, disinfection byproducts (DBP)

3.2 Introduction

Ozone (O_3) is a strong oxidant used in drinking water, aquaculture, and potentially in ballast water treatment applications. However, O_3 reacts with bromide ions (Br^-) to create toxic byproducts such as bromine (Br_2), hypobromite ion (OBr^-), hypobromous acid (HOBr), bromoform ($CHBr_3$), and bromate (BrO_3^-) (Kim et al., 2007; Song et al.,

1996; von Gunten and Hoigne, 1994). Bromide ions are naturally present in seawater and are also found in drinking water sources. Of growing concern is the potential increase of salt-water intrusion in coastal area aquifers due to predicted sea level rise (Bonacquisti, 2006; Butler et al., 2005), leading to unwanted occurrence of bromide in coastal source waters. Further, bromide can also be present in inland sources due to geological composites or upstream industrial effluents (von Gunten and Hoigne, 1994).

The USEPA (2009) has identified bromate as a contaminant that increases the risk of cancer and have set a maximum contaminant level (MCL) of 0.010 mgL^{-1} for drinking water, with a MCL goal (MCLG) of reducing this limit to zero. Compliance with the MCLG for bromate will become increasingly difficult for water treatment plants where bromide exists in the source water and ozone is used as the disinfectant. Although there are methods to control the formation of bromate during ozonation (Hofmann and Andrews, 2001), controlling bromate formation in bromide rich waters is a challenge and an identified research need for the desalination industry (Agus et al., 2009). Additionally, due to the carcinogenic properties of bromate and other brominated DBP, it is possible that these unwanted byproducts will impact the health of fish in aquaculture and marine environments (Tango and Gagnon, 2003).

Detection of bromate in drinking water is normally through the use of ion chromatography (US EPA Method 317) or inductively coupled plasma mass spectrometry (ICP-MS) (US EPA Method 321.8). These accepted analytical methods are often inadequate in saline or brackish water systems, as other abundant anions (e.g., chloride) interfere with the detection of bromate. As noted by Fukushi et al. (2009), there are limited methods to detect bromate in brackish water and thus there is need to develop methodologies for monitoring bromate for brackish water.

The objective of this chapter was to develop a simple and accurate method for the measurement of bromate in various water matrices that can be used in drinking water, ballast water, and aquaculture applications. The study specifically produced a spectrophotometric method that does not require costly and complex analytical

equipment, generates results in a timely fashion, and would not be subject to interfering anions (e.g. chloride).

3.3 Materials and Methods

3.3.1 Water Matrices

In total, seven water matrices were used to test the method and are presented in Table 1. Seawater and artificial brackish water were prepared as described in section 2.1.To compare raw water sources with treated waters, tap water from Halifax Regional Municipality having a chlorine residual > 0.2 mgL^{-1}, dechlorinated tap water, and laboratory grade Milli-Q water were tested.

Table 1. Water quality characteristics of sources studied.

ID	Source	Salinity (mg/L)	Conductivity (µS/cm)	DOC (mg/L)	Bromide (mg/L)
MQ	Milli-Q Water	0.00E+00	2.2	0	0
Tap	J.D. Kline WTP Halifax, NS	0.00E+00	88.6	0	0
DCl	Dechlorinated Tap Water Halifax, NS	0.00E+00	89.4	0	0
SB	Lake Rodney Shelburne, NS	0.00E+00	25.8	12.2	0
Tat	French River Tatamagouche, NS	0.00E+00	97.4	2.0	0
SW	Seawater Halifax Harbour, NS	3.00E+04	40400	--	44
BR	50% French River/50% Seawater	1.50E+04	24200	4.6	22

3.3.2 Equipment

A Hach Model DR/5000 (Loveland, CO) UV-spectrophotometer and 1 cm glass cuvette were used for absorbance measurements. Bromate concentrations were verified by ion chromatography (IC) according to USEPA Method 300.1 (1999). The method detection limit (MDL) for bromate was 5 μgL^{-1}.

3.3.3 Reagents

Milli-Q water and analytical-reagent grade chemicals were used. $NaBrO_3$ (Spex CertiPrep, Metuchen, NJ) was spiked into 200 mL of each water matrix to produce stock solutions at the desired concentrations. A 0.1 M glycine buffer solution of pH 1.0 was prepared from glycine (Fisher Scientific, Toronto, ON) and hydrochloric acid. Lastly, a 1.0 M iodide solution was prepared with NaI (Fisher Scientific, Toronto, ON).

3.3.4 Procedure

For each water matrix, 200 mL stock solutions of 0.01, 0.5, 1.0, 3.0, and 5.0 mgL^{-1} bromate were prepared. All water samples were passed through a 0.45 μm filter prior to stock solution preparation. In addition, quality control stock solutions of 0.04, 0.15, 0.25, 2.0, and 3.5 mgL^{-1} were prepared for each water matrix, tested using the spectrophotometric method, and checked by ion chromatography.

As shown in Figure 5, 2 mL of 0.1 M glycine buffer having pH 1.0, and 1 mL of 1.0 M iodide was mixed with 7 mL of bromate-spiked stock solution. The 10 mL solution was shaken and allowed to sit for a reaction time of 5 minutes. Once the reaction was complete, a 1 cm cuvette was filled and tested for UV absorbance at a wavelength of 352 nm. To verify the bromate concentration of all bromate-spiked stock solutions, 7 mL of each stock solution was mixed with 3 mL of Milli-Q water and measured by ion chromatography.

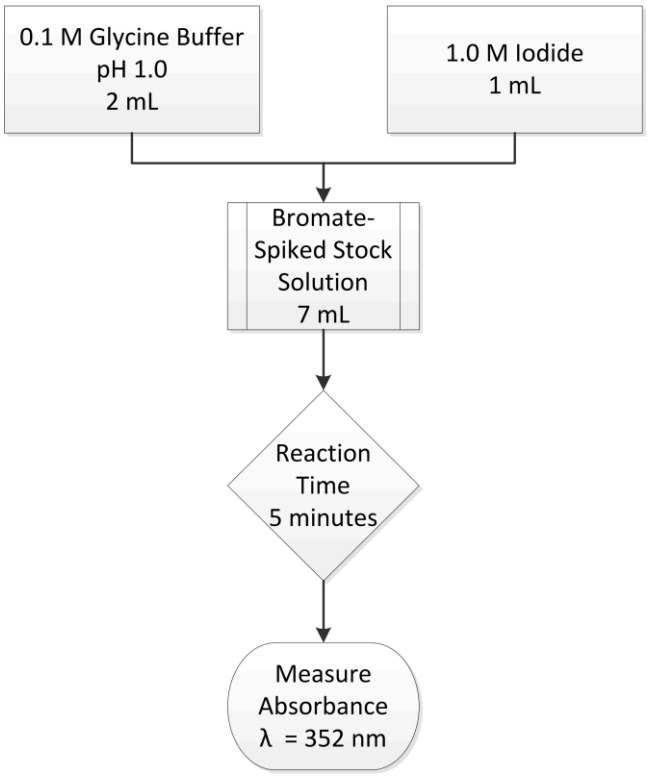

Figure 5. Procedure of the spectrophotometric method used to determine bromate concentration.

3.3.5 Statistical and Data Analysis

The method was performed on each water matrix four times for each concentration of bromate. Quality control points were tested in duplicate. The method detection limits were determined according to the procedure described by Berthouex and Brown (1994) that uses the proportionality of the Student's *t* value for a 99% confidence level and the standard deviation of seven replicate absorbance values for a concentration of 3 mgL^{-1} bromate for each water matrix. Reaction times were evaluated by performing the Student's *t* test at the 99% confidence level. By performing the F-Test at the 99% confidence level, the variance throughout each model was determined to be statistically insignificant.

3.4 Results and Discussion

3.4.1 Reaction Chemistry

Afkhami et al., (2001) proposed a spectrophotometric method for determining the periodate, iodate, and bromate mixtures that was based on their reaction with iodide. The reaction occurs at pH 1.0 and the tri-iodide produced is monitored by the resulting UV_{352} absorbance.

$$BrO_3^- + 9I^- + 6H^+ \Leftrightarrow 3I_3^- + Br^- + 3H_2O \qquad (1)$$

Afkhami et al., (2001) noted that bromate did not completely react with iodide during the three minute reaction time of their method. This was also observed in the present study, and resulted in testing five minute and ten minute reaction times. The absorbance values observed after ten minutes were not statistically different from those observed after five minutes. Thus, this method uses a reaction time of five minutes, as it was determined to be sufficient for the bromate and iodide to fully react. Afkhami et al., (2001) also acknowledged that the induction period of the reaction was dependent upon both pH and concentration of the reagents. Thus, by using a 1.0 M iodide reagent at pH 1.0, the reaction of bromate and iodide occurs more quickly and completely than reported by Afkhami et al., (2001). A greater concentration of iodide was used to ensure that it would not be exhausted by bromate during the longer reaction time.

3.4.2 Effect of Bromate Concentration

As previously described in section 2.4, bromate was spiked into each of the water matrices at concentrations in the range of 0.05 – 5.0 mgL^{-1}. For each matrix, UV_{352} was proportional to the concentration of bromate, allowing a linear model to be produced and calibrated. Figure 6 illustrates bromate concentration in Milli-Q water and the corresponding absorbance for each concentration. For Milli-Q water a linear regression having an $R^2 > 0.99$ between UV_{352} absorbance and bromate concentration was observed. Thus, the method could calculate the concentration of bromate based on the observed absorbance.

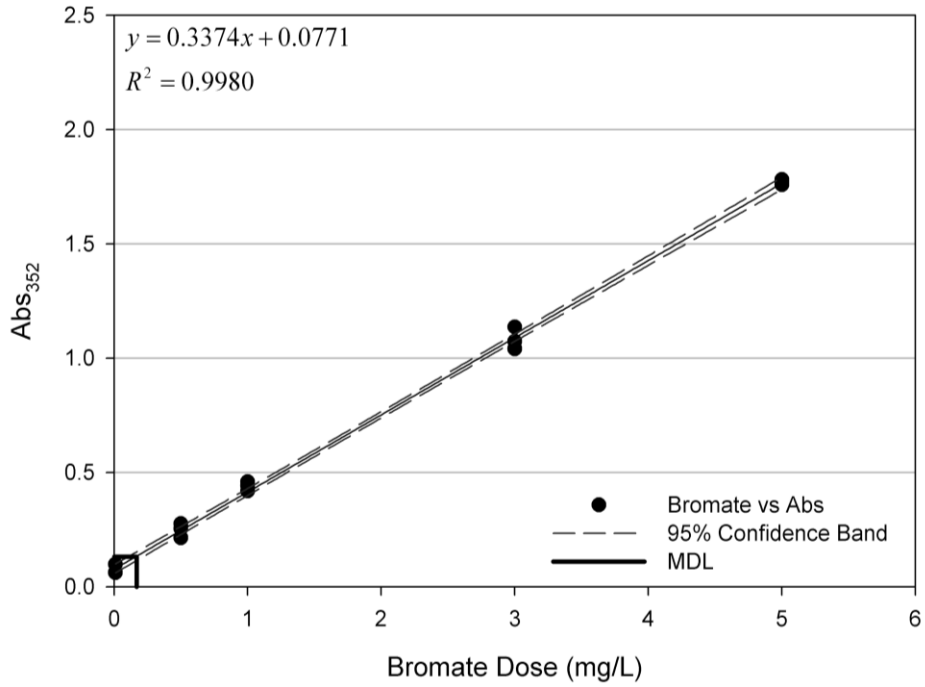

Figure 6. Bromate concentration in Milli-Q water is calculated based on the observed absorbance.

Figure 7 and Figure 8 illustrate that by using the described method, bromate concentrations can be determined in more complex water matrices, such as brackish water and seawater, respectively. As observed in Table 2, slope of the model decreased at higher salinity concentrations. This is attributed to the increased anionic demand on the iodide. As salinity increased from brackish water to seawater, less iodide was available to react with brome, which resulted in less tri-iodide formed, therefore a lower UV_{352} absorption was observed. Despite the presence of chloride ions and the change in slope, bromate was accurately determined in both brackish water and seawater.

Table 2. Spectrophotometric models for the detection of bromate.

Source	Linear Model	R^2	MDL (mg/L)
Milli-Q	Abs_{352}=0.3374Bromate+0.0771	0.9980	0.16
Tap	Abs_{352}=0.3169Bromate+0.0901	0.9806	0.32
Dechlorinated Tap	Abs_{352}=0.3126Bromate+0.0867	0.9871	0.39
Shelburne	Abs_{352}=0.3375Bromate+0.0495	0.9692	0.18
Tatamagouche	Abs_{352}=0.3249Bromate+0.1468	0.9923	0.20
Brackish	Abs_{352}=0.2580Bromate+0.0681	0.9925	0.31
Seawater	Abs_{352}=0.1909Bromate+0.0430	0.9856	0.14

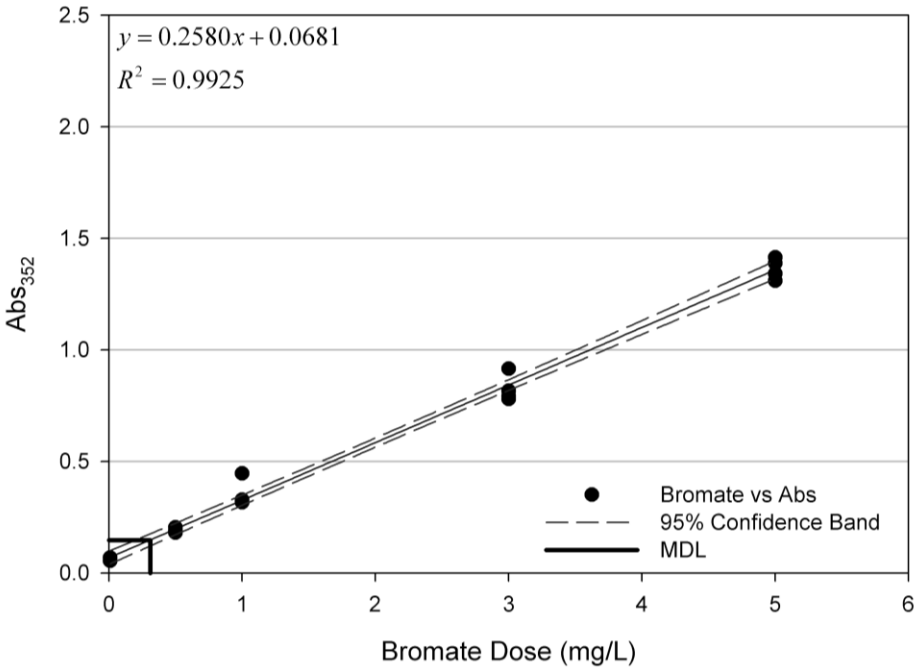

Figure 7. Bromate concentration in brackish water is calculated based on the observed absorbance despite the presence of DOC, bromide, and chloride ions.

Additional fresh water matrices were tested and the results are also presented in Table 2. The linear model for each water matrix has an $R^2 > 0.95$, and MDL < 0.4 mgL^{-1} bromate. In spiked water samples, Fukushi et al. (2009) developed a different UV-spectrophotometric approach and reported a sample recovery of greater than 99% for samples with a bromate concentration greater than 0.5 mgL^{-1}. However the sample recovery decreased to 85% for bromate concentration of 0.25mgL^{-1} and MDLs were not

reported by Fukushi et al. (2009). The MDL for the present study and potentially for the method presented by Fukushi et al. (2009) exceeds the current MCL for bromate of $0.01 mgL^{-1}$. Thus the described method is not suitable for routine monitoring of drinking water for regulatory purposes. However, the described method would be appropriately applied for detecting background bromate concentrations in saline systems in which other interfering anions (e.g., chloride) mask the detection of bromate through traditional analytical methods.

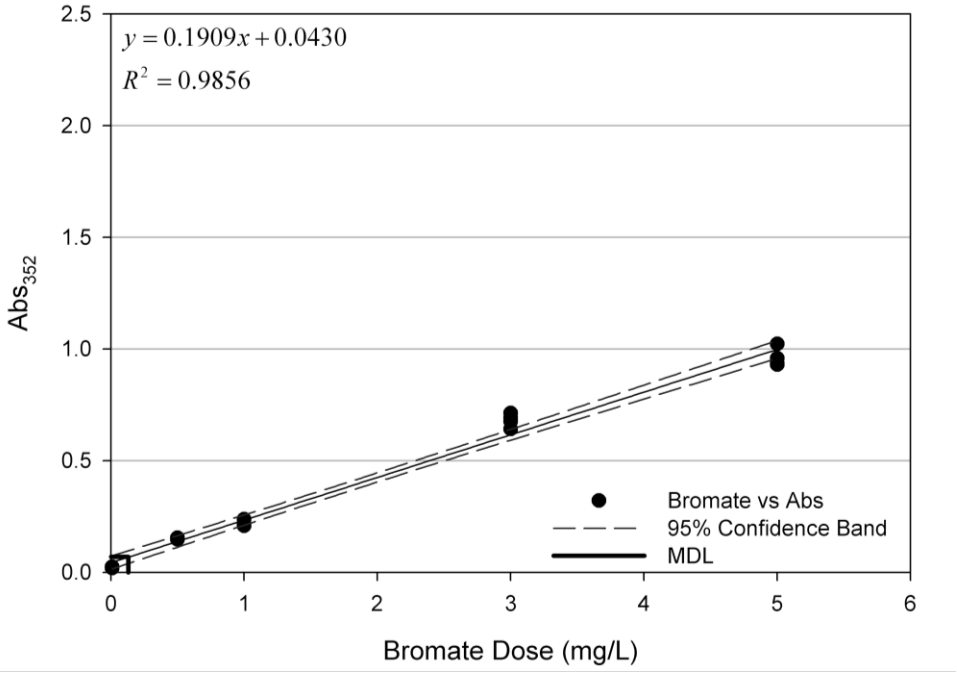

Figure 8. Bromate concentration in seawater is calculated based on the observed absorbance despite the high concentration of chloride ions present in seawater.

3.4.3 Method Accuracy

The bromate concentrations in each water matrix were analyzed by ion chromatography to verify the accuracy of the method. Figure 9 shows the bromate concentration measured by ion chromatography versus the concentration calculated by the model. The linear regression model having a slope of 0.9583 and an $R^2 > 0.99$ demonstrates the accuracy of the model.

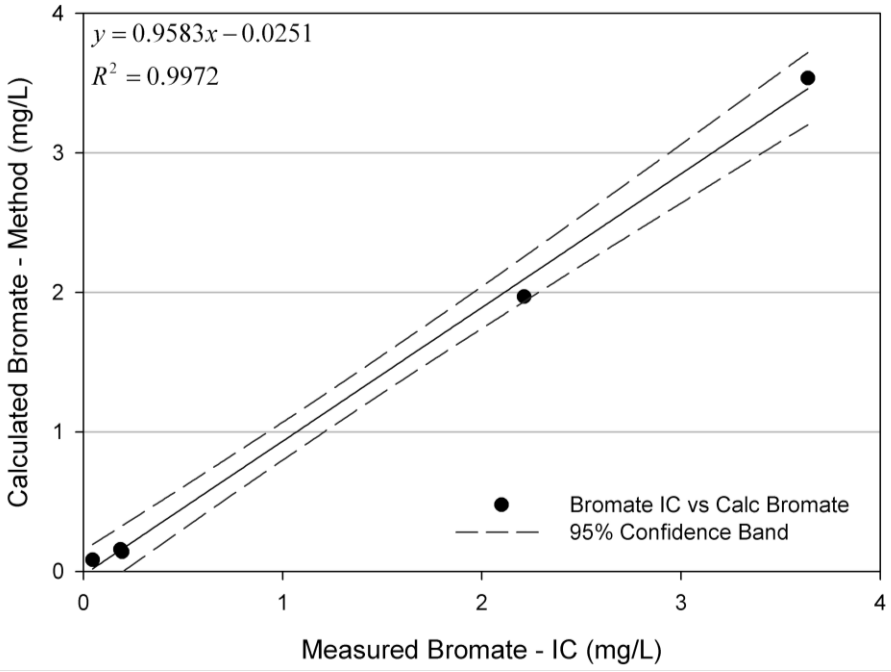

Figure 9. Bromate concentrations calculated by the observed absorbances lie within the 95% confidence band.

3.5 Conclusion

This study set out to develop a fast, simple, and accurate method for the determination of bromate concentration in a wide range of water matrices. As bromate becomes more rigidly controlled and monitored, having the ability to quickly and accurately measure the concentration will prove useful. Bromate was spiked into a wide range of water matrices, from laboratory grade Milli-Q water to synthetic brackish water composed of seawater and freshwater having high DOC. The method described herein quickly and accurately determined the concentration of bromate in both simple and complex water matrices using common laboratory equipment.

Chapter 4 Comparing Formation of Bromate and Bromoform Due to Ozonation and UV-TiO_2 Oxidation in Saline Waters

* A modified version of this Chapter was submitted to the *Journal of Advanced Oxidation Technologies* in July 2010
Co-authored by Rupa Lamsal and Graham Gagnon.
Author provided the major contribution to this manuscript.

4.1 Abstract

The objective of this study was to compare bromate formation between ozonation and suspended titanium dioxide (TiO_2) disinfection of brackish water, and to study the physical and chemical sustainability of TiO_2 nanoparticles in oxidation processes. The study was carried out in bench scale using a collimated beam for ultraviolet (UV) light and an ozone generator that utilized the corona discharge method to form ozone. Seawater was used for photocatalysis and ozonation experiments to relate bromate formation to aquaculture applications. Artificial brackish water was used to relate bromate formation to drinking water sources that face seawater intrusion. Physical changes to the nanoparticles were analyzed by taking scanning electron microscope (SEM) images before and after exposure to UV and water. Chemical changes to the nanoparticles were analyzed by comparing x-ray photoelectron spectroscopy (XPS) spectra before and after photocatalysis. Trihalomethanes and bromate were measured to evaluate the potential of UV-TiO_2 or ozone for producing these disinfectant by-products (DBPs). A key finding from the study was that disinfection by UV-TiO_2 produced a lower concentration of DBPs than disinfection by ozone. In particular, this study found that ozonation produced up to 4.5 mgL^{-1} of bromate, whereas UV-TiO_2 did not produce bromate at detectable concentrations (<5 μgL^{-1}) in any of the water matrices studied. Bromoform concentrations after disinfection by ozone were as high as 148 μgL^{-1}, but after disinfection by UV-TiO_2 bromoform was below the detection limit (<5.9 μgL^{-1}) for the water matrices studied. Furthermore, other DBP precursor levels were consistently

lower in UV-TiO_2 experiments than in ozonation trials. Overall, this study highlights the promise of UV-TiO_2 photocatalysis as a future disinfection method in various water treatment applications.

KEY WORDS: titanium dioxide, nanoparticles, bromoform, ozone, ballast water, DBP

4.2 Introduction

Titanium dioxide (TiO_2) nanoparticles have several applications, including photocatalysis. Studies indicate that ultraviolet disinfection processes in drinking water are synergistically enhanced using TiO_2 nanoparticles in combination with low-pressure UV light (Gerrity et al., 2008; Ryu et al., 2008). Furthermore, titanium dioxide nanoparticles have been used in advanced oxidation applications to successfully treat various environmental pollutants, such as bacteria, viruses, and dissolved organic matter attributed to the formation of THM in water (Cho et al., 2005; Hand et al., 1995).

Ozone (O_3) is a strong oxidant used in drinking water, aquaculture, and potentially, in ballast water treatment applications. However, O_3 reacts with bromide ions (Br^-) to create toxic byproducts such as bromine (Br_2), hypobromite ion (OBr^-), hypobromous acid (HOBr), bromoform ($CHBr_3$), and bromate (BrO_3^-). Bromide ions are naturally present in seawater and are found in drinking water sources. Salt water intrusion in coastal area aquifers may increase due to predicted sea level rise (Bonacquisti, 2006; Butler et al., 2005), and will lead to unwanted occurrence of bromide in coastal source waters. Further, bromide can also be present in inland sources due to geological composites or upstream industrial effluents (von Gunten and Hoigne, 1994). Artificial brackish water was used in this study to examine the DBP formation potential in a drinking water matrix that had been contaminated with saline water. While the authors acknowledge that drinking water will not have 15 ppt salinity, this was chosen to illustrate the ability of UV-TiO_2 to oxidize without forming brominated DBPs in an environment that promotes DBP formation.

The USEPA (2009) has identified bromate as a contaminant that increases the risk of cancer, and have set a maximum contaminant level (MCL) of 0.010 mgL^{-1} for drinking water, with a goal (MCLG) of reducing this limit to zero. Compliance with the MCLG for bromate will become increasingly difficult for water treatment plants where bromide exists in the source water. Tercero Espinoza and Frimmel (2008) found UV irradiation of suspended titanium dioxide nanoparticles did not produce bromate in brominated drinking water.

The overall objective of this project was to compare disinfectant byproduct formation from O_3 and TiO_2 disinfection processes in saline water collected from Halifax Harbour in Halifax, Nova Scotia, Canada and to physically characterize titanium dioxide nanoparticles following UV irradiation. The project specifically examined bromate and trihalomethane (THM) formation as a result of TiO_2 photocatalysis and ozonation under controlled laboratory conditions.

4.3 Materials and Methods

4.3.1 Disinfection

Seawater and brackish water were prepared as described in section 2.1. UV irradiation of Degussa P25 anatase TiO_2 nanoparticles was conducted according the procedure outlined in section 2.2. Ozonation of samples was achieved using the bench scale semi-batch apparatus shown and described in section 2.3. Ozonation times were chosen such that treatment duration would be similar for both O_3 and UV-TiO_2 disinfection. The resulting ozone Ct (concentration x time) values have been shown to achieve less than 1.5 log inactivation of *Cryptosporidium parvum* (Craik et al., 2003; Rennecker et al., 1999).

4.3.2 Sample Analyses

TiO_2 nanoparticles were analyzed before and after photocatalysis for both physical and chemical changes. Physical changes were analyzed by SEM imaging (section 2.4), and analysis of chemical changes was performed by XPS as discussed in section 2.5.

4.3.3 Experimental Design

Photocatalysis experiments had three test parameters: Br^- concentration, TiO_2 concentration, and UV fluence. Br^- concentration of the seawater was determined to be 44 mgL^{-1}. Typical Br^- concentration of seawater is 67 mgL^{-1} (Perrins et al., 2006), so to encourage bromate formation during photocatalysis, samples were spiked with NaBr (Spex CertiPrep, Metuchen, NJ) to achieve 75 mgL^{-1} Br^-. Seawater was combined with water from the French River in Tatamagouche, Nova Scotia to produce artificial brackish water having Br^- concentration of 22 mgL^{-1}. Suspended TiO_2 nanoparticles have proven to be effective photo-oxidants at 1 and 10 mgL^{-1} (Gerrity et al., 2008), but higher concentrations cause the slurry to become too milky for complete photoactivation of the TiO_2. Consequently, the target photocatalyst concentrations were 1, 5, and 10 mgL^{-1}. To achieve 2.0 log inactivation of viruses using UV treatment, the EPA requires drinking water treatment plants to administer a dose of 100 mJ/cm^2 of UV light, but only 5.2 and 5.8 mJ/cm^2 to achieve the same inactivation of *Giardia* and *Cryptosporidium*, respectively (USEPA, 2006). In Australia, the minimum microbicidal dose is 40 mJ/cm^2 (Cabaj et al., 1996), thus 5, 50, and 100 mJ/cm^2 were used as the UV fluence settings.

4.3.4 Disinfection Byproducts

Analysis of the DBP formation as a result of both ozone and TiO_2 photocatalysis was performed according to section 2.6. Bromate and bromoform were the disinfection byproducts measured.

4.3.5 Statistical and Data Analysis

All experiments were conducted in duplicate, and in random order. Statistically significant results were determined with the student *t* test at the 95% confidence level.

4.4 Results and Discussion

4.4.1 TiO_2 Does Not Significantly Reduce Bromide Concentration

Increasing TiO_2 concentration from 1 mgL^{-1} to 10 mgL^{-1} increased the recovered Br^- concentration by an average of 8 mgL^{-1} (Figure 10). For experiments involving TiO_2 at a concentration of 10 mgL^{-1}, the water turned "milky" allowing less of the nanoparticles to

be irradiated by the UV light because of light shielding. Under these light shielding situations, it has been observed that fewer hydroxyl radicals are produced to react with bromide to form $BrOH^-$ (von Gunten and Hoigne, 1994). Gerrity et al. (2008) also found that higher TiO_2 concentrations (i.e., greater than 10 mgL^{-1}) reduced photoactivity through light shielding.

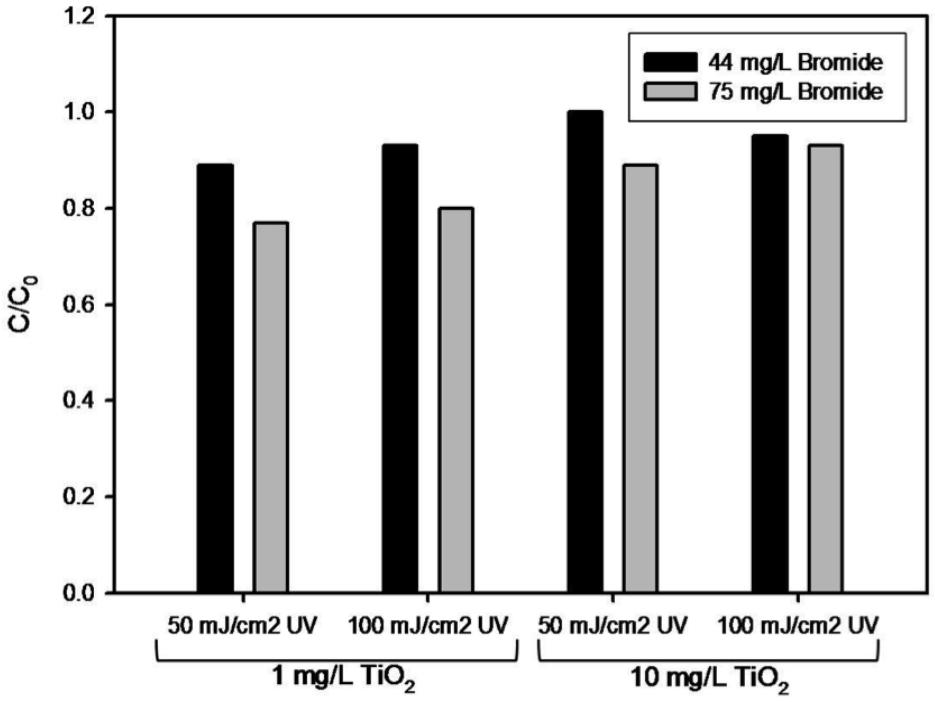

Figure 10. Concentration of bromide after photocatalysis increases as TiO_2 concentration increases due to light shielding.

4.4.2 TiO_2 Disinfects Without Increasing ORP

Ozone disinfection of seawater increased ORP nearly nine times the initial level (from 50 to 475 mV) during 120 minutes of ozonation (60 mgL^{-1} ozone), which creates a toxic environment for aquatic species such as fish in discharge areas or aquaculture applications. In contrast, TiO_2 photocatalysis decreased the ORP by 15% (Figure 11) during 120 minutes of irradiation. The reduction, found to be statistically different at the 95% confidence level, is an example of how photocatalysis disinfects without the negative effects that accompany ozonation. The drastic difference is due to the formation of hypobromous acid and hypobromite during ozonation. The intermediary and secondary reactants had a concentration of approximately 3 mgL^{-1} in the ozone trials.

These secondary disinfectants are not produced during photocatalysis, thus they do not contribute to the ORP. The disinfection mechanism in photocatalysis is the production of hydroxyl radicals (•OH) and superoxide radicals ($•O_2^-$) (Gerrity et al., 2008), which do not affect ORP.

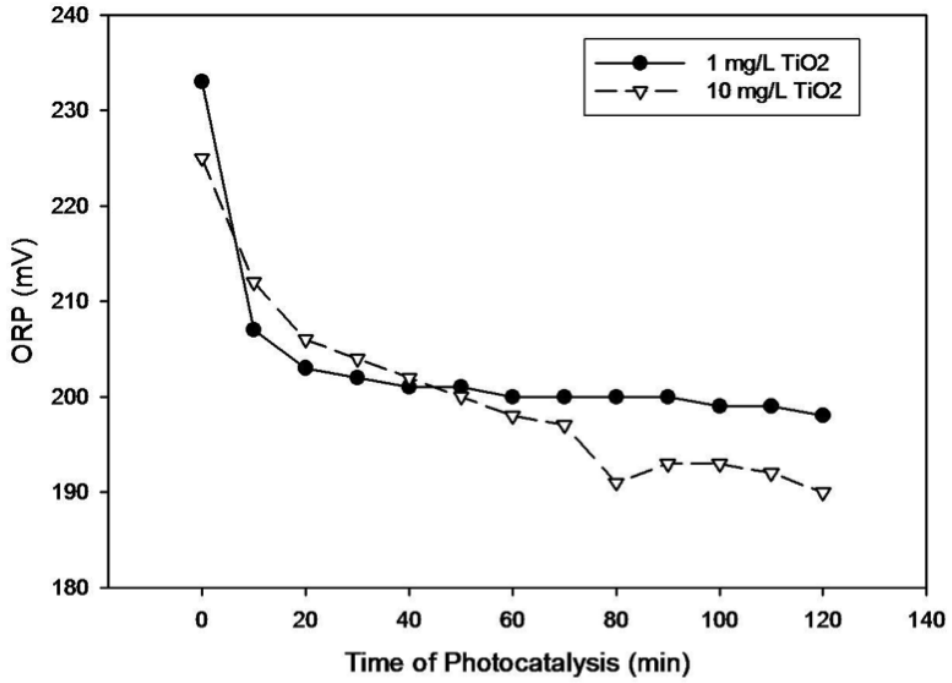

Figure 11. Oxidation-reduction potential (ORP) decreases during photocatalysis.

4.4.3 Bromate Formation is Not Observed Following UV-TiO_2 Oxidation

It is well noted in literature that O_3 reacts with Br^- ions to create BrO_3^- (Song et al., 1996; von Gunten, 2003a; von Gunten and Hoigne, 1994; Westerhoff et al., 1998). Hypobromite (OBr^-) is required, along with bromide and ozone, for the formation of bromate. Hypobromite accumulates as a primary intermediate in solutions containing bromide and ozone (von Gunten and Hoigne, 1994). Disinfection by UV-TiO_2 occurs primarily as a result of hydroxyl radical production. It is reported that when halides such as Br^- are photo-oxidized by TiO_2, the final products are Br_2^-, Br, or Br^- (Fitzmaurice et al., 1993; Henglein, 1982; Linsebigler et al., 1995; Moser and Gratzel, 1982). Thus bromate was not detected after treatment by UV-TiO_2 (). Treatment with ozone at all doses (0.4 – 3.9 mgL^{-1} ozone) formed bromate levels well beyond that of the MCL of 10 μgL^{-1} (USEPA, 2009). Due to the carcinogenic properties of bromate and other brominated DBP, it is possible that these unwanted byproducts will impact the health of

fish in aquaculture and ballast water environments (Tango and Gagnon, 2003). It is unrealistic to treat seawater or highly brackish water with ozone alone and expect to meet drinking water standards. However, the ability to meet the bromate MCLG of zero μgL^{-1} in the same waters with UV-TiO_2 treatment is significant and warrants further investigation of this technology.

4.4.4 Bromoform is Controlled by UV-TiO_2 Oxidation

During ozonation of water containing bromide, HOBr and OBr^- are intermediate and secondary disinfectants that are formed, as well as $CHBr_3$ (von Gunten, 2003b). Bromoform is a trihalomethane (THM), which is a regulated byproduct in drinking water. The USEPA (2009) requires all drinking water to contain less than 80 μgL^{-1} of total THM. Dissolved organic carbon (DOC) concentration plays a significant role in the formation of bromo-organic compounds. In a study of 38 ozone treatment plants, the only one to contain significant levels of bromoform had a very high concentration of DOC > 6 mgL^{-1} (Legube, 1996). The samples in this study had concentrations of DOC being 2.5 and 4.6 mgL^{-1} for seawater and brackish water, respectively. Ozonation produces bromoform that exceeds the MCL in brackish water, and significant levels of bromoform in seawater. Ozonation of brackish water produces more bromoform than seawater due to the increased DOC. Treatment with UV-TiO_2 does not produce bromoform at detectable levels in the same water matrices (). The ability of UV-TiO_2 treatment to disinfect without producing THM demonstrates the potential of this method for both aquaculture and drinking water applications.

Table 3. Bromate and bromoform formed due to oxidation.

Sample				THM (µg/L)					Bromate (mg/L)
Salinity (ppt)	TiO_2 (mg/L)	UV (mJ/cm^2)	Ozone CT (mg min/L)	Chloroform	Dichlorobromo-methane	Dibromochloro-methane	Bromoform	Total THM	
15	1	5		0	0	0	0	0	0.0
15	1	50		0	0	0	0	0	0.0
15	5	5		0	0	0	0	0	0.0
15	5	50		0	0	0	0	0	0.0
30	1	5		0	0	0	0	0	0.0
30	1	50		0	0	0	0	0	0.0
30	5	5		0	0	0	0	0	0.0
30	5	50		0	0	0	0	0	0.0
15			0.4	0	1	4	146	151	0.4
15			1.0	0	2	4	148	154	1.0
15			1.9	0	1	4	121	126	1.7
15			3.9	0	2	3	22	27	2.0
30			0.4	0	2	3	28	33	0.5
30			1.0	0	1	3	26	29	1.2
30			1.9	0	2	3	26	31	2.9
30			3.9	0	1	3	18	22	4.5

4.4.5 TiO_2 Nanoparticles are Physically and Chemically Stable in Water Treatment Processes

The synergistic benefits of TiO_2 photocatalysis for water treatment are well documented, such as enhanced bacterial and viral disinfection (Cho et al., 2005; Gerrity et al., 2008) and reduction of trihalomethane precursor material (Liu et al., 2008). As such, it is clear that this disinfection method will eventually be a practical treatment option for various industries. It is imperative that new and innovative techniques be developed and implemented with sustainability in mind. The clearest theoretical advantage of photocatalysis to UV treatment alone is the reduction in contact time required to achieve a level of disinfection. This directly translates into less power consumption per unit of water treated (Bottero et al., 2006). This study also examined the physical and chemical characteristics of TiO_2 nanoparticles following photocatalysis. Figure 12 shows the TiO_2 nanoparticles in their commercially packaged state. The particles were approximately 25 nm in diameter. Consistent with previous works (Cabrera et al., 1996), the nanoparticles were observed in larger agglomerates that ranged in size from 0.7 to 0.9 μm in diameter.

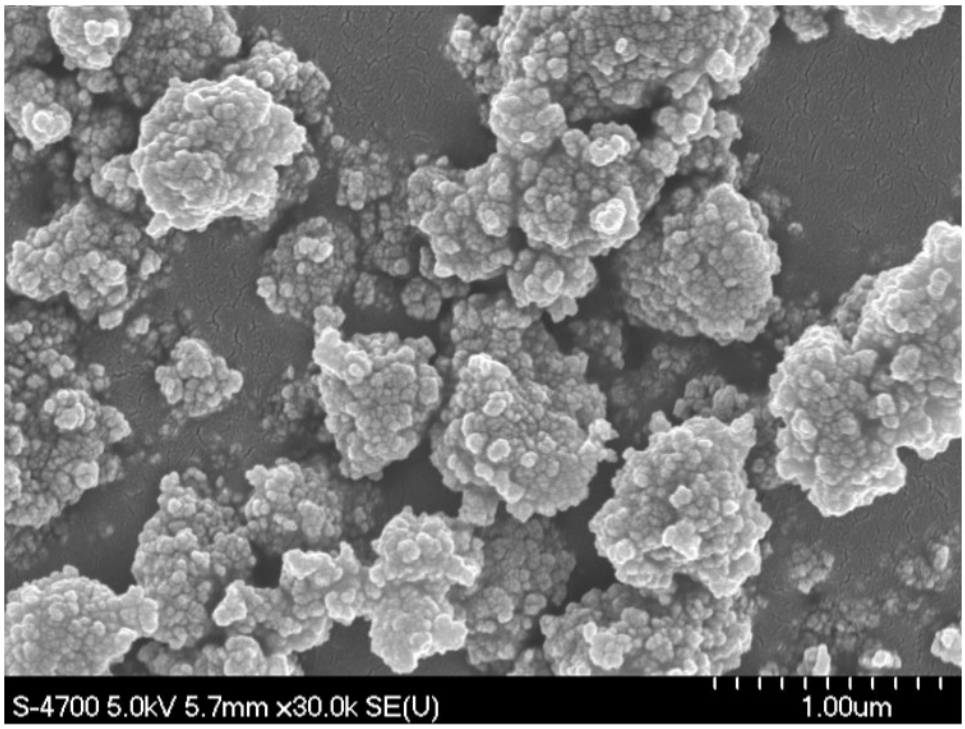

Figure 12. SEM image of Degussa P25 TiO_2 nanoparticles in their commercial state.

Upon slow stirring during UV irradiation and filtration afterwards, the agglomerate sizes increased in size, as expected (Balasubramanian et al., 2003; Erdem et al., 2001). However, physical changes to the nanoparticles were not observed after low or high dose irradiation in either water matrix (Figure 13 and Figure 14).

During photocatalysis of TiO_2 having a bandgap energy of 3.2 eV, electrons were excited by UV light (λ=253.7 nm) from the valence band into the conduction band. Positively charged holes (h^+) in the valence band produce hydroxyl radicals (OH•) by oxidizing water or hydroxide ions. The electrons excited to the conduction band (e^-_{TiO2}) reduce oxygen to superoxide radicals (O_2^-•). The radicals formed are known as reactive oxygen species (ROS) and have significant disinfection and oxidation properties. In addition, UV irradiation produces surface defect sites (Ti^{3+}), or oxygen vacancies (Gopel et al., 1983). Oxygen adsorbs to the defect sites, thus producing O_2^- and subsequent formation of hydroxyl groups (Gopel et al., 1983; Linsebigler et al., 1995). The defect sites created by UV irradiation are partly responsible for the oxidation-reduction properties of TiO_2 (Linsebigler et al., 1995). The photocatalytic activity of TiO_2 is completed and, in fact, enhanced by an increase of hydroxyl content on the surface (Yu et al., 2000).

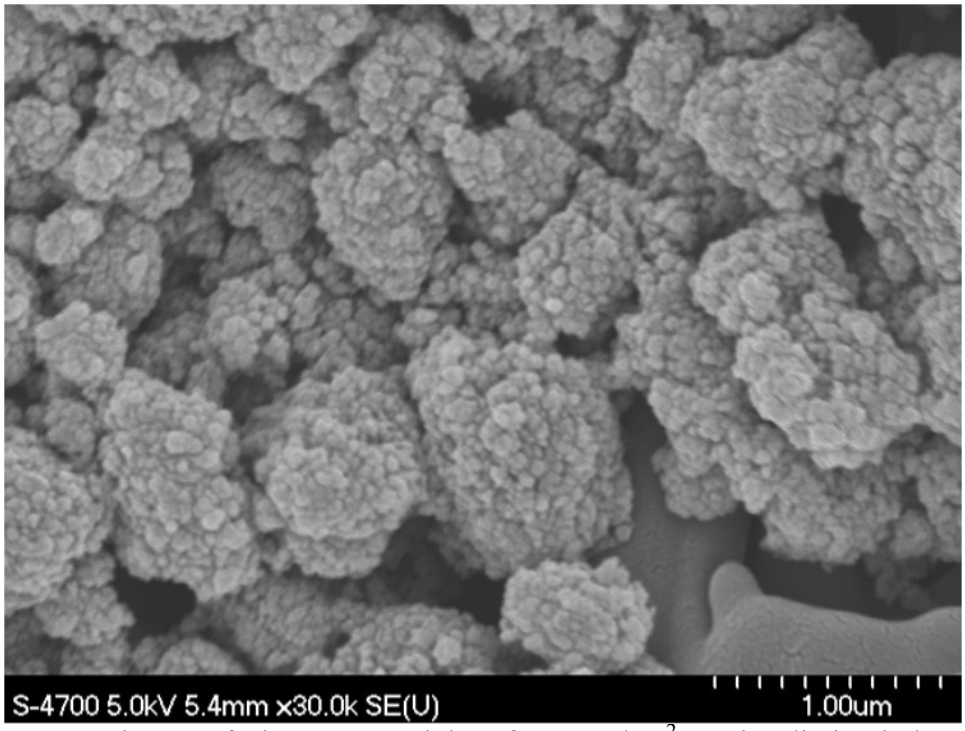

Figure 13. SEM image of TiO_2 nanoparticles after 5 mJ/cm^2 UV irradiation in brackish water.

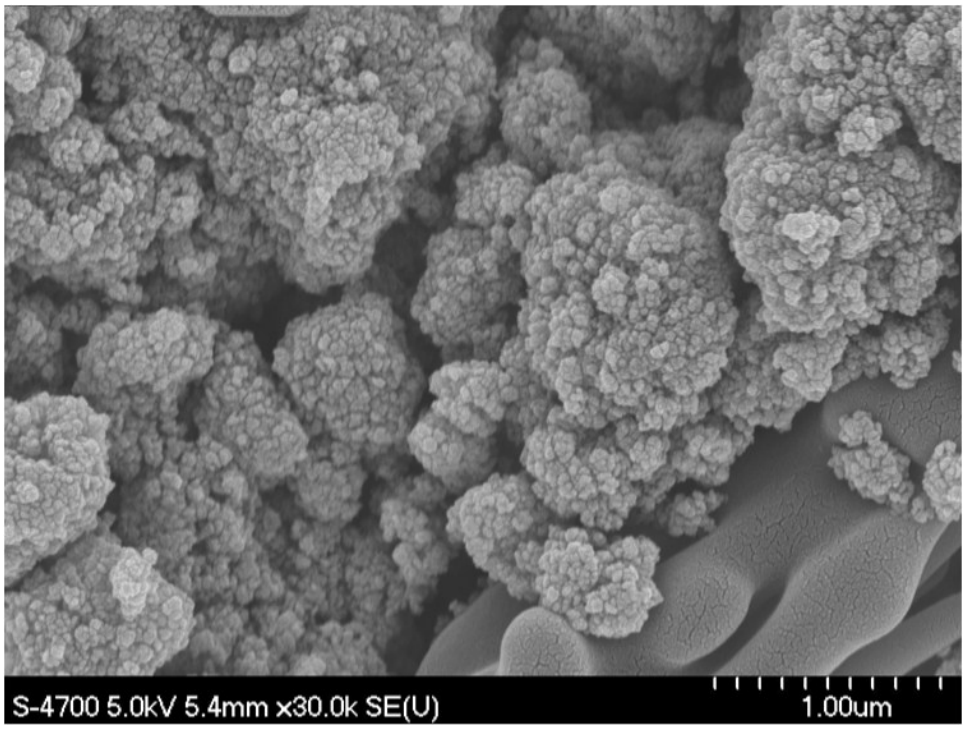

Figure 14. SEM image of TiO_2 nanoparticles after 50 mJ/cm2 UV irradiation in seawater.

The chemical state of the TiO_2 nanoparticles was studied by XPS before and after irradiation. The low-resolution spectra confirmed that the nanoparticles were titanium dioxide. High-resolution spectra comparison of the Ti2p peaks after UV irradiation shows a broadening of the peaks and a shoulder located on the lower binding energy side (Figure 15). These are similar to results observed by Wang et al. (1999) and are attributed to the Ti^{3+} defect state. The high-resolution spectra comparison of the O1s peaks after UV irradiation also shows a broadening of the peaks and a shoulder located on the side of lower binding energy (Figure 16). Wang et al. (1999) associated the shoulder band located approximately 1.5 eV below the O1s band to hydroxyl groups adsorbed to the surface, and further concluded that defect sites are more favorable to hydroxyl adsorption than oxygen adsorption. During the photocatalytic process, the concentration of electrons surpasses that of photogenerated holes due to the relatively slow charge transfer to adsorbed molecular oxygen (Gerischer, 1993; Linsebigler et al., 1995). As hydroxyl groups replace oxygen at the defect sites, the electron concentration increases at the surface forming an accumulation layer that is characterized by a reduction of the electron potential energy. This can be seen by the shift of both Ti2p and O1s peaks approximately 0.5 eV towards lower binding energies (Figure 17 and Figure 18). Thus the shift indicates simply that hydroxyl groups have replaced adsorbed oxygen on the surface, which readily reacts with holes (h^+) to produce hydroxyl radicals.

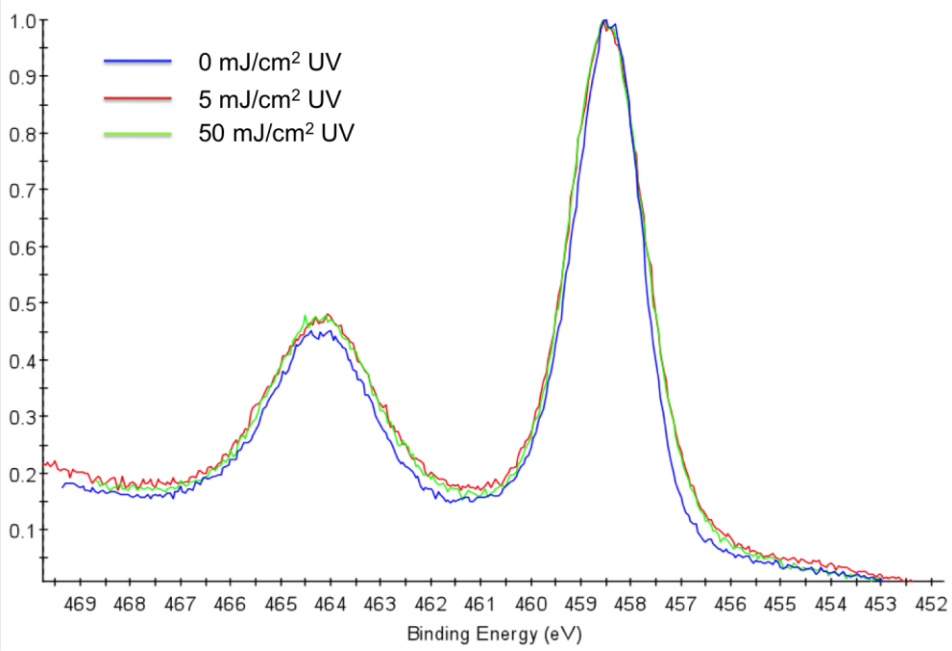

Figure 15. High-resolution XPS spectra comparison of the Ti2p peak.

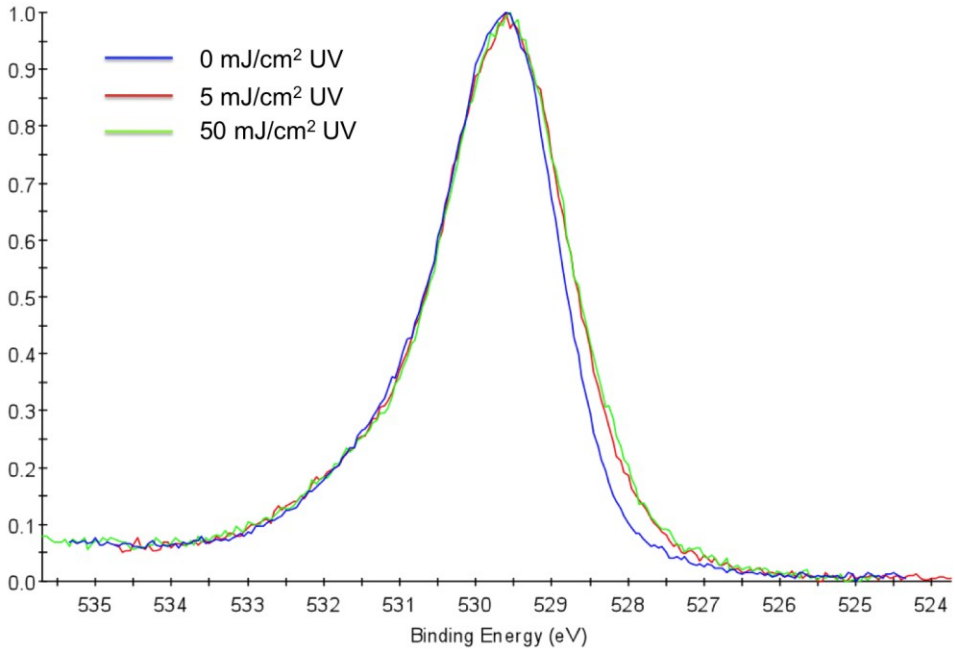

Figure 16. High-resolution XPS spectra comparison of the O1s peak.

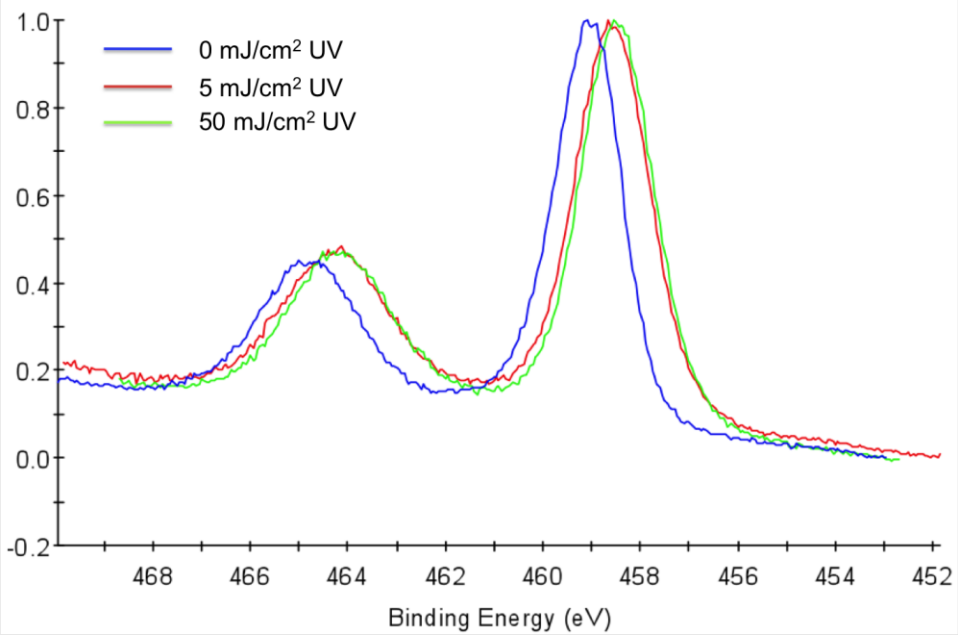

Figure 17. High-resolution spectra comparison of the Ti2p peak shows that UV-irradiated nanoparticles shifted 0.5 eV towards lower binding energies.

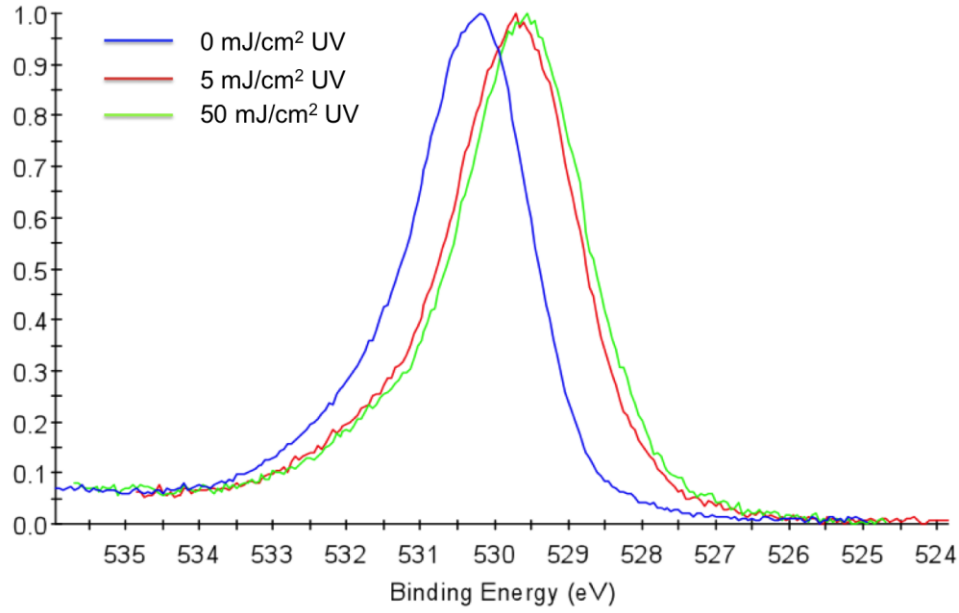

Figure 18. High-resolution XPS spectra comparison of the O1s peak shows that UV-irradiated nanoparticles shifted 0.5 eV towards lower binding energies.

The difference in Ti2p peaks before and after UV irradition observed in Figure 15 is attributed to the Ti^{3+} defect state created by the exposure to UV light (Shultz et al., 1995). However, Shultz et al. (1995) and Wang et al. (1995; 1999) reported that XPS is unable distinguish between a defect-free surface and a surface that was healed by oxygen or hydroxyl groups. Analysis of TiO_2 by XPS is useful for indirect, qualitative detection of •OH production. However, due to the many variables and uncertainties involved with the technique and its results, a direct method for the detection of •OH would provide additional credibility to the findings.

4.5 Conclusion

This study set out to compare bromate formation in ozone and UV-TiO_2 disinfection of water containing bromide. As an emerging technology in the water treatment industry, TiO_2 photocatalysis could have several applications for water treatment. Despite favorable conditions for bromate and other DBP formation, brominated byproducts were not detected as a result of TiO_2 photocatalysis. Bromide concentrations were not significantly reduced and secondary disinfectants, OBr^- and HOBr, were not formed during photocatalysis. This illustrates that bromide ions are mostly unaffected during UV-TiO_2 oxidation. It was confirmed through physical and chemical analyses of the TiO_2 nanoparticles that formation of OH• from TiO_2 was generated. As noted in the literature, OH• do not lead to the formation of bromate. Alternatively, ozonation of the same water matrices formed OBr^- and HOBr, which further reacted with ozone to produce bromate and bromoform at levels above the USEPA Maximum Contaminant Levels. UV-TiO_2 oxidation has shown the ability meet the USEPA Maximum Contaminant Level Goals for bromate and bromoform. TiO_2 nanoparticles were found to be physically and chemically stable and sustainable when used in an advanced oxidation process in the water treatment industry.

Chapter 5 Photocatalytic Hydroxyl Radical Production by Titanium Dioxide Nanostructured Thin Film Support

5.1 Abstract

Two forms of titanium dioxide were analyzed for the photocatalytic production of hydroxyl radicals by low pressure UV light. Suspended anatase TiO_2 nanoparticles were compared to TiO_2 supported on 3M Company's nanostructured thin film (NSTF) by magnetron sputter deposition. Hydroxyl radical (•OH) production was analyzed by the degradation of *para*-chlorobenzoic acid (pCBA), a common •OH probe compound. Sputtered TiO_2 on NSTF was found to be comparable to suspended anatase TiO_2, producing •OH on the order of 10^{-15} M.

KEY WORDS: hydroxyl radicals, pCBA, HPLC, TiO_2 nanoparticles, NSTF

5.2 Introduction

Titanium dioxide (TiO_2) nanoparticles have been the focus of an extensive body of research related to their photocatalytic disinfection properties. TiO_2 nanoparticles have been used in advanced oxidation applications to successfully treat various environmental pollutants in water, including bacteria (Cho et al., 2004), viruses (Gerrity et al., 2008), pesticides (Sanches et al., 2010), and dissolved organic matter attributed to the formation of THM in water (Hand et al., 1995). Disinfection by TiO_2 nanoparticles is achieved through production of hydroxyl radicals that are highly non-selective, and react readily with organic material (Brunet et al., 2009).

Although TiO_2 nanoparticles are effective for disinfection, they must be removed from suspension in the water after the photocatalytic process (Thiruvenkatachari et al., 2008). This represents a significant challenge associated with commercial TiO_2/UV reactor designs, as the uncertainty in releasing TiO_2 into the environment, or recapturing of the

catalyst have been constraints in practical design and application. The concentration of suspended TiO_2 is limited to 10 mgL^{-1} for disinfection due to light shielding (Gerrity et al., 2008), in which fewer nanoparticles are irradiated, therefore producing fewer hydroxyl radicals. Additionally, fewer organisms are exposed to the UV light resulting in reduced disinfection when compared to lower TiO_2 concentrations.

To alleviate these constraints, this project studies magnetron sputter deposition of TiO_2 onto an advanced polyimide nanostructured thin film (NSTF) support manufactured by 3M Company (St. Paul, MN) for its ability to produce hydroxyl radicals in water. NSTF has a very high surface area, approximately 10 – 15 times greater than other films (Debe, 2003), which allows more TiO_2 reaction sites without altering the transmittance of the water. *Para*-chlorobenzoic acid, (pCBA) is a commonly used probe compound for the detection of •OH in water (Brunet et al., 2009; Cho et al., 2005; Elovitz and von Gunten, 1999; Pi et al., 2005; Watts and Linden, 2007). The use of x-ray photoelectron spectroscopy (XPS) to indirectly detect the formation of •OH by examining the surface defects of TiO_2 that result from UV irradiation, as conducted in the previous chapter, is useful but complicated and limited by several factors (Shultz et al., 1995; Wang et al., 1995; Wang et al., 1999). Thus, pCBA was used to compare •OH formation by TiO_2-sputtered NSTF (TiO_2-NSTF) and suspended Degussa P25 anatase titanium (IV) oxide nanopowder (99.7% trace metals basis, Sigma Aldrich, St. Louis, MO). The degradation of pCBA was compared to evaluate the water treatment potential of this innovative catalyst stabilization technique.

5.3 Materials and Methods

5.3.1 TiO_2 on Nanostructured Thin Film Support (NSTF) Support

Debe et al. (2003; 1995; 1994) describes the production and characterization of nanostructured thin film (NSTF) catalyst supports developed by 3M Company (St. Paul, MN) for use in the fuel cell industry. The NSTF, shown in Figure 19, consists of 3 to 5 billion crystalline organic pigment support whiskers per cm^2 attached to an advanced polyimide carrier sheet that can be coated with any desired material

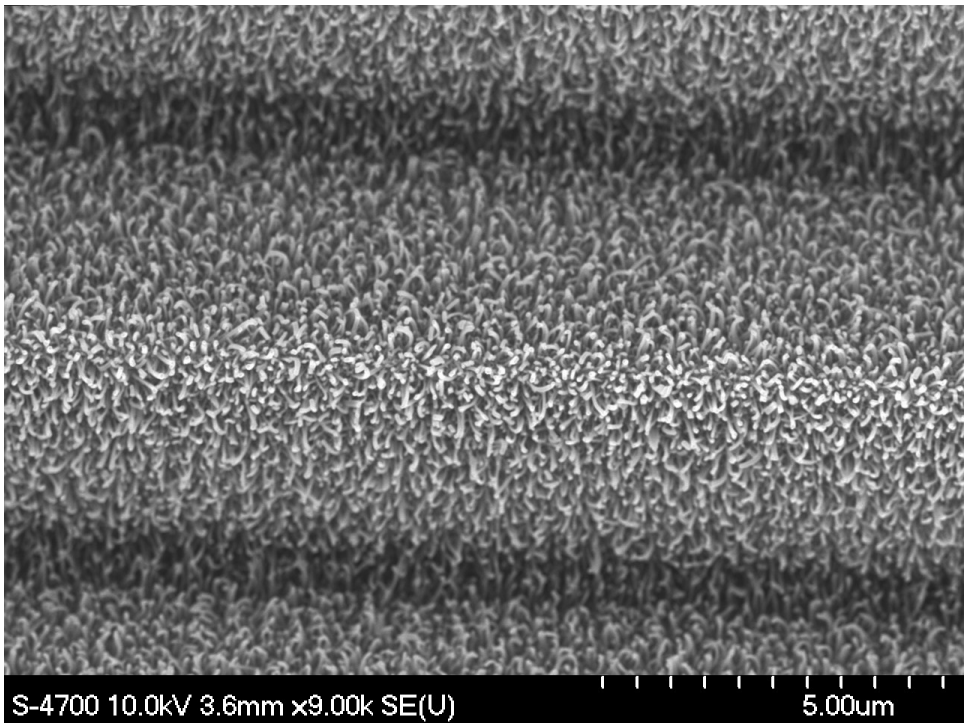

Figure 19. Nanostructured thin film (NSTF) produced by 3M Company (St. Paul, MN) has a very high surface area due to 3 to 5 billion whiskers per cm^2.

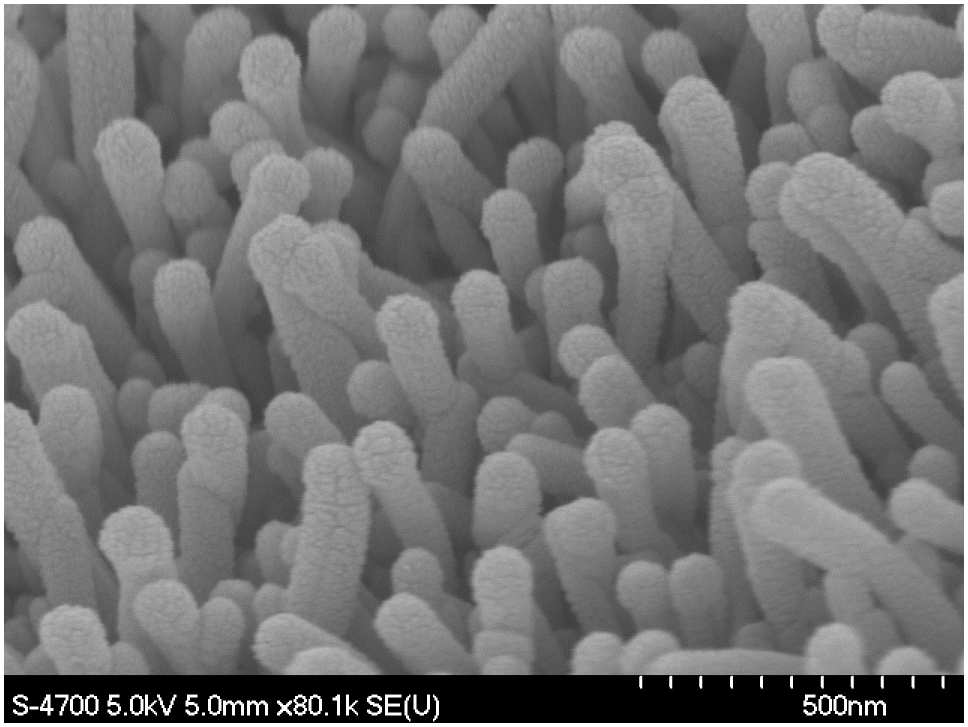

Figure 20. NSTF whiskers coated with 300 nm planar equivalent TiO_2 by magnetron sputter deposition.

(Bonakdarpour et al., 2008; Dahn et al., 2002; Debe, 2003; Debe and Drube, 1995; Debe and Poirier, 1994). For this study, NSTF was coated with titanium dioxide by magnetron sputter deposition as described by Dahn et al. (2002) using two titanium dioxide targets and constant mask openings. The depositions produced catalyst-coated whisker films with a planar loading equivalent of 300 nm or 0.125 mg TiO_2 cm^{-2} (Figure 20). The sputtered TiO_2 is suspected to be amorphous.

5.3.2 Analysis of pCBA

Milli-Q water was spiked with 25 µM *para*-chlorobenzoic acid (pCBA) (Sigma Aldrich, St. Louis, MO), a highly specific probe compound that is degraded in the presence of hydroxyl radicals (Cho et al., 2004; Elovitz and von Gunten, 1999; Pereira et al., 2007; Sanches et al., 2010). Samples were collected after exposure to TiO_2 and 100, 500, and 1500 mJ/cm^2 UV doses to indirectly test for the presence of •OH radicals by monitoring the degradation of pCBA. The concentration of pCBA was analyzed by high performance liquid chromatography (HPLC) according to section 2.7.

5.3.3 UV-TiO_2 Photocatalysis

The samples were dosed with suspended TiO_2 nanoparticles or pieces of TiO_2-coated NSTF. Samples were irradiated using a low pressure UV lamp in a collimated beam (Trojan Technologies, London, ON) as discussed in section 2.2.

5.3.4 X-ray Photoelectron Spectroscopy (XPS)

To confirm the deposition on the NSTF was TiO_2, and to investigate the photocatalytic production of hydroxyl radicals by the catalyst on the NSTF whiskers, the samples were analyzed by x-ray photoelectron spectroscopy as previously described in section 2.5.

5.4 Results and Discussion

5.4.1 XPS Analysis of NSTF

NSTF was coated by magnetron sputter deposition with bulk titanium targets in the presence of oxygen under vacuum conditions. To determine that the deposition on the NSTF was, in fact, titanium dioxide and not a different titanium oxide species, XPS analysis of the resulting film was performed. As illustrated in Figure 21, the O1s peak located at approximately 529 eV, and the $Ti2p_{3/2}$ peak located at approximately 458 eV suggest that there is approximately double the amount of oxygen as titanium present on the surface of the NSTF.

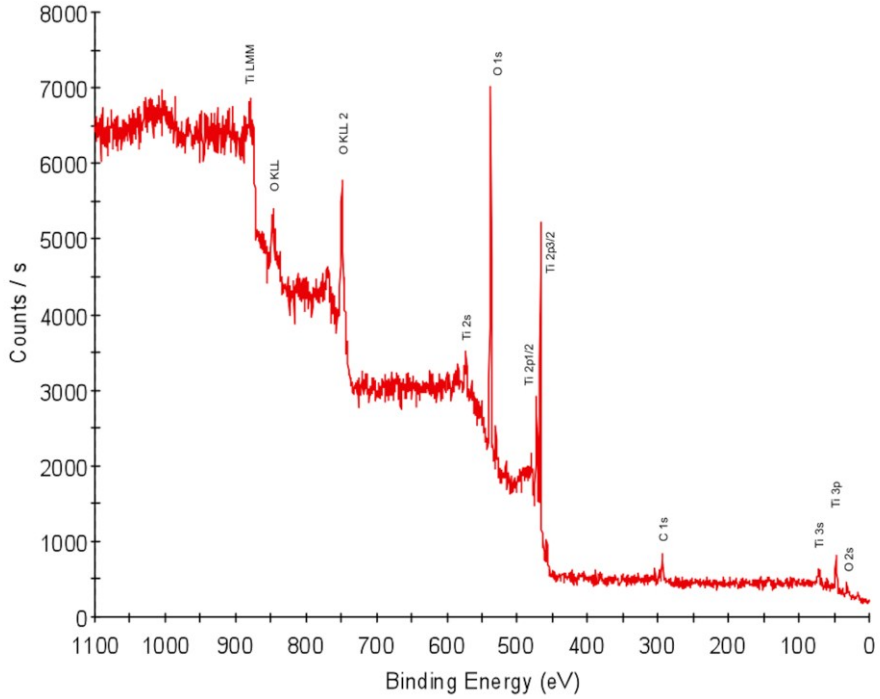

Figure 21. XPS analysis of sputtered NSTF suggests titanium dioxide (TiO_2) is present.

5.4.2 ICP/MS Results

Various freshwater matrices were analyzed for titanium by ICP/MS after four months exposure to NSTF sputtered with TiO_2 that resulted in a concentration of 1 mgL^{-1} of TiO_2 in each sample. Titanium was not detected (detection limit is 2 μgL^{-1}) in Milli-Q, tap and dechlorinated tap water from Halifax Regional Municipality in Nova Scotia, and raw water from the French River in Tatamagouche, Nova Scotia. Brackish water and

seawater were also tested. The detection limit was 20 μgL^{-1} due to the increased complexity of the water matrix. Titanium was not detected in the saline samples. However, up to 4 μgL^{-1} titanium (detection limit is 2 μgL^{-1}) was detected in raw water from Rodney Lake near Shelburne, Nova Scotia. Control samples were not analyzed because titanium was not expected to be present, even at trace levels. The detected titanium in the Shelburne sample is believed to be a result of a reported iron ore deposit near Shelburne that consists of large amounts of titanium (Gilpin Jr. and Engineers, 2009), and not a result of exposure to TiO_2-NSTF. Future analyses of control samples will clarify this hypothesis.

5.4.3 Bromate Formation

Seawater and brackish water were analyzed after photocatalysis by TiO_2-NSTF for bromate and bromoform production. Brackish water had a salinity of 15 ppt, and 22 mgL^{-1} bromide, while seawater had a salinity of 30 ppt, and 44 mgL^{-1} bromide. Similar to the results presented in sections 4.4.3 and 4.4.4 for suspended TiO_2 photocatalysis in the same water matrices, no bromate or bromoform were observed as a result of TiO_2-NSTF disinfection.

5.4.4 pCBA Degradation

Irradiation of TiO_2 nanoparticles by UV light forms reactive oxygen species, including hydroxyl radicals which are highly non-specific, but have a very brief lifetime of approximately 10 µs (Brunet et al., 2009). *Para*-chlorobenzoic acid reacts readily with hydroxyl radicals, and is thus used as a probe compound (Cho et al., 2004; Cho and Yoon, 2008; Elovitz and von Gunten, 1999; Pi et al., 2005). In this study, pCBA was degraded (significant at 95% confidence level) by both concentrations of suspended TiO_2 nanopowder when exposed to UV fluences of 500 and 1500 mJ/cm^2. As well, both concentrations of TiO_2-NSTF degraded pCBA significantly when exposed to 1500 mJ/cm^2, but only 1 mgL^{-1} TiO_2-NSTF showed significant pCBA degradation at 500 mJ/cm^2.

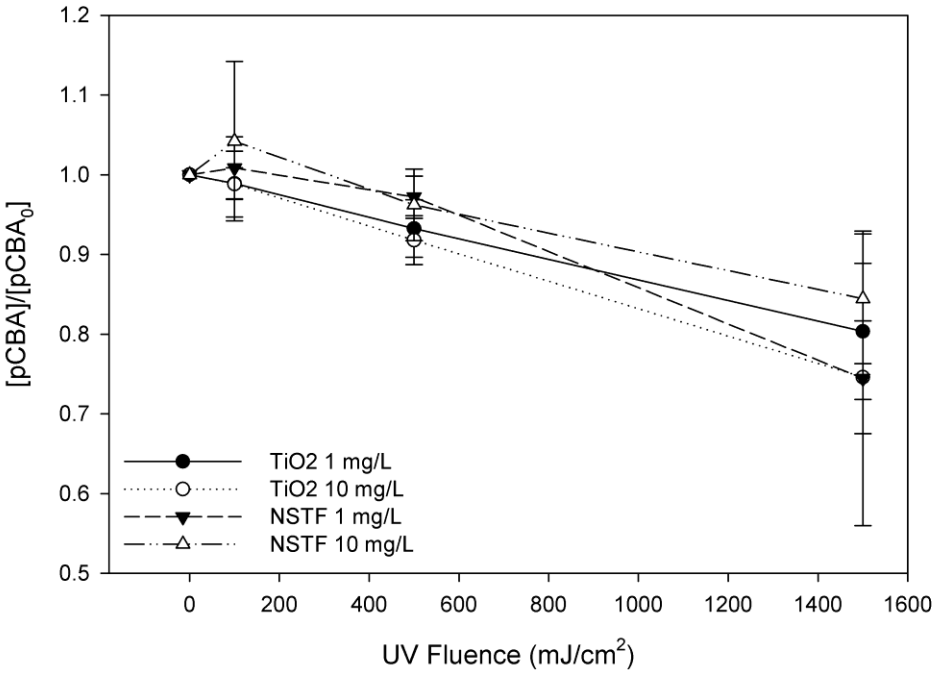

Figure 22. pCBA degradation by TiO_2 supported on NSTF is similar to that of suspended anatase TiO_2 nanoparticles. Error bars represent 95% confidence intervals.

In studies involving TiO_2 photocatalysis, Cho et al., (2004; 2008) expressed the degradation of pCBA by •OH as:

$$-\frac{d[pCBA]}{dt} = k_{\bullet OH/pCBA}[pCBA][\bullet OH] \quad (2)$$

Integration yields:

$$-\ln\left(\frac{[pCBA]}{[pCBA]_0}\right) = k^* t \quad (3)$$

where, if the pseudo-steady-state assumption for the •OH is valid, the net rate coefficient is:

$$k^* = k_{\bullet OH/pCBA}[\bullet OH] \quad (4)$$

Neta and Dorfman (1968) reported $k_{\bullet OH/pCBA} = 5 \times 10^9\ M^{-1}s^{-1}$, which allows •OH concentration to be calculated using Equation 2 (Cho et al., 2004; Cho and Yoon, 2008).

In this study, as in Cho et al., (2004) and Cho and Yoon, (2008), k^* was determined from the slope of the line following a regression analysis of the plot of pCBA degradation and time (t), according to Equation 3. Constant pCBA degradation (linear relationship having $R^2 > 0.95$ for all trials) confirms the pseudo-steady-state assumption for the •OH concentration (Cho et al., 2004; Cho and Yoon, 2008).

Constant pCBA degradation was observed as a result of all photocatalytic experiments (1 mgL^{-1} suspended TiO_2 shown in Figure 23). Thus, the pseudo-steady-state concentration of •OH is present, and the net rate coefficient, k^*, can be used to calculate the steady-state •OH concentration from Equations 2 and 4 (Cho and Yoon, 2008; Neta and Dorfman, 1968).

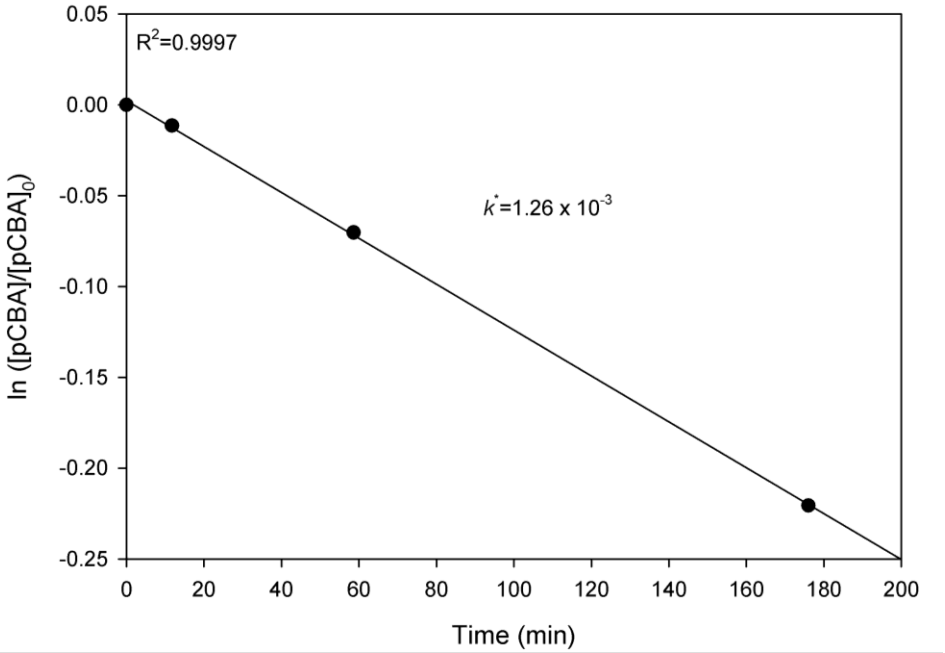

Figure 23. Photocatalytic degradation of pCBA by •OH produced by 1 mgL^{-1} suspended TiO_2.

Table 4. k^* values and •OH concentrations produced by suspended TiO_2 and TiO_2-NSTF.

Type	[TiO_2] mg/L	k^*	R^2	[•OH] mg/L	[•OH] M
Suspended	1	1.26×10^{-3}	0.9997	7.1×10^{-11}	4.2×10^{-15}
Suspended	10	1.63×10^{-3}	0.9982	9.2×10^{-11}	5.4×10^{-15}
NSTF	1	1.83×10^{-3}	0.9610	1.0×10^{-10}	6.1×10^{-15}
NSTF	10	1.26×10^{-3}	0.9504	7.1×10^{-11}	4.2×10^{-15}

Table 4 lists the k^* values and the concentrations of hydroxyl radicals produced by suspended TiO_2 and TiO_2-NSTF. The k^* values represent the net rate coefficient for each photocatalytic process. The hydroxyl radical production does not increase linearly with suspended TiO_2 concentration. This is likely due to increased light shielding resulting from additional particles in suspension blocking others, thus inhibiting •OH production. Hydroxyl radical production by TiO_2-NSTF is higher at 1 mgL^{-1} than at 10 mgL^{-1}. It is possible that there is a scavenging effect of hydroxyl radicals by the polymer material that composes the NSTF. TiO_2-NSTF concentrations were determined by the size of NSTF coupon added to the water sample. All NSTF coupons had a planar equivalent thickness of 300 nm, 0.125 mg/cm^2, TiO_2. The 1 mgL^{-1} TiO_2-NSTF coupons were 0.36 cm^2, and the 10 mgL^{-1} TiO_2-NSTF coupons were 4.0 cm^2. The increased amount of polymer in the samples may have impacted the pCBA degradation.

Similar production of •OH by TiO_2 supported on NSTF to that of suspended TiO_2 nanoparticles was observed. Both immobilized and suspended TiO_2, at each concentration studied, produced a steady-state •OH concentration on the order of 10^{-15} M. This concentration is two orders of magnitude lower than the •OH concentration reported by Elovitz and von Gunten (1999) as a result of ozonation in a completely different water matrix. The disparity is likely due to the different level of pCBA used, and the ozone concentration of 20-25 μM. However, the production of ozone is a very energy-intensive process when compared to using a low-pressure UV lamp. The advantage of NSTF in the water industry is that the benefits of TiO_2 photocatalysis may be practically realized.

5.5 Conclusion

Increased pCBA degradation has been reported when the pCBA concentration is orders of magnitude lower(Cho et al., 2004; Cho and Yoon, 2008; Sanches et al., 2010), or suspended TiO_2 concentration (Cho et al., 2004; Cho and Yoon, 2008) or UV fluence (Brunet et al., 2009) is greatly increased when compared to parameters used in this study. However, the purpose of this study was to compare the potential of sputtered TiO_2-NSTF as a suitable photocatalyst to conventional suspended TiO_2 by evaluating the production of hydroxyl radicals. It was found that all [•OH] are on the order of 10^{-15} M, illustrating that TiO_2 supported on NSTF is equally suitable for production of hydroxyl radicals as suspended anatase TiO_2 for water treatment purposes. By using a low-pressure UV lamp and TiO_2 immobilized on NSTF, •OH were produced and there were no suspended particles that required removal. TiO_2 immobilized on NSTF by magnetron sputter deposition warrants further investigation for use as a low-energy water treatment technology.

Chapter 6 Conclusion

6.1 Synthesis

The work presented in this thesis was conducted to evaluate the potential of a new water treatment technology in which proven UV disinfection is integrated with 3M Company's novel nanomaterials coated with TiO_2. The potential was evaluated by monitoring DBP formation, comparing •OH production to suspended TiO_2, and analyzing the TiO_2 on the NSTF for changes due to UV irradiation (shown in Appendix D). Additionally, water samples were studied to determine if TiO_2 deposited on the NSTF had become dissociated with the film and had entered the water matrix. A method for detecting bromate in saline water was also developed

The results obtained and included in this thesis contribute to the overall objective; to develop an innovative water treatment technology that incorporates UV technology and 3M Company's NSTF coated with TiO_2 without forming bromate or other DBPs. When irradiated under low-pressure UV light, TiO_2 immobilized on 3M Company's NSTF produces •OH on the order of 10^{-15} M, similar to that of suspended TiO_2 nanoparticles. Bromate formation was not detected as a DBP of suspended TiO_2 or TiO_2-NSTF photocatalysis in any water matrix. The use of NSTF as a support for TiO_2 during photocatalysis has emerged as an innovative advanced oxidation process that disinfects without forming regulated DBPs, namely bromate, in various water matrices. The emergence of this water treatment technology meets the primary objective of this thesis.

6.2 Conclusions

The use of UV technology in the water treatment industry is well established. UV reactors have small footprints, are capable of achieving the required level of disinfection for multiple pathogens, and do not produce unwanted DBPs. Due to the widespread use of UV technology already in place throughout the water treatment industry, a successful photocatalyst, such as NSTF coated with TiO_2, could be easily implemented to provide improved treatment.

6.2.1 Controlling Bromate Formation

Bromate formation was monitored in all UV-TiO_2 experiments, as well as ozonation experiments. Ozone, as expected, produced bromate at concentrations above regulated limits. All UV-TiO_2 experiments, however, did not produce bromate or bromoform at detectable levels. UV doses up to 1500 mJ/cm^2 and TiO_2 doses up to 10 mgL^{-1} were analyzed without detection of any brominated DBPs. The ability to disinfect a wide variety of source waters (i.e., freshwater with NOM, brackish water, or seawater) without forming regulated DBPs by UV-TiO_2 technologies could have a significant impact on the water treatment industry. This research has shown that both suspended TiO_2 nanoparticles and TiO_2 supported on NSTF do not produce bromate or bromoform in freshwater, brackish water, or seawater.

6.2.2 Monitoring Bromate Formation in Saline Systems

A known reaction between iodide and bromate at low pH was exploited to develop a new method to measure bromate indirectly. The benefit of this method is that once a specific water matrix is calibrated, the concentration of bromate can be measured very quickly by a UV spectrophotometer, common in most water laboratories. Bromate reacts with the added iodide at low pH, and the concentration of bromate is then calculated by the change in absorbance measured at 352 nm wavelengths. The method was developed and tested on seven different water matrices; five freshwater, one brackish water, and one seawater. Each water matrix had a different linear model that calculated concentration of bromate. Once this model was created, the bromate concentration could accurately be determined in minutes.

The method's detection levels are higher than the maximum bromate allowed in drinking water, which limits its use for drinking water. However, the method could be used to quickly monitor high concentrations of bromate. If none is detected by the spectrophotometric method, then analysis by ion chromatography would be conducted to detect lower concentrations in drinking water. For the marine aquaculture industry,

where ozone is commonly used in recirculation systems, bromate can quickly be monitored using this new method.

6.2.3 Applying Innovative Nanotechnology to Water Treatment

Nanotechnology is a rapidly growing industry that consists of the development and modification of materials that characteristically are sized on the order of 10^{-9} to 10^{-6} meters. One of the many applications of nanotechnology is the use of photoactive particles that synergistically enhance the inactivation of organisms by UV light in water. The most studied photocatalyst in for water treatment is titanium dioxide due to its ability to produce highly reactive hydroxyl radicals in water when excited by UV light. While the production of hydroxyl radicals is very beneficial for disinfection, having to remove the suspended nanoparticles after disinfection is not practical.

Magnetron sputter deposition of TiO_2 onto NSTF support was determined to be equally as efficient at photocatalytic hydroxyl radical production as suspended anatase TiO_2 nanoparticles. Both methods of introducing TiO_2 to the water and UV light produced the highly non-specific hydroxyl radicals on the order of 10^{-15} M. The ability of sputtered TiO_2 supported on NSTF to produce hydroxyl radicals in the same manner as suspended nanoparticle TiO_2 is important to photocatalyst research. Additionally, the NSTF appeared to be unchanged after UV exposure when examined by SEM. Lastly, photocatalysis of TiO_2, whether suspended or deposited on NSTF, did not produce bromate or bromoform at detectable levels. While the results presented here are elementary, they provide a basis warranting further research on NSTF as a support for photocatalysts to be practically integrated into water treatment.

6.3 Recommendations

TiO_2 photocatalysis has been heavily studied for its benefits to water treatment. The major drawback that has kept it from being widely used is the required removal of suspended particles. Many studies exploring the possible methods of immobilizing TiO_2

for use in photocatalysis have been presented. This thesis presents another method of TiO_2 immobilization and the potential of this method as an advanced oxidation process.

6.3.1 Continue Evaluation of NSTF in Photocatalytic Environments

Degradation of pCBA as an indirect measure of •OH production was performed and presented in Chapter 5. Additional pCBA degradation trials should be performed using NSTF coupons that have the same area, but differ in TiO_2 thickness to achieve the desired concentration of TiO_2. This would exploit the benefits of the high surface area of NSTF and help to evaluate the role of the NSTF support as a potential •OH scavenger. The effect of prolonged exposure of NSTF to •OH should also be evaluated.

6.3.2 Monitor DBP Formation Potential

The formation of bromate and bromoform were monitored throughout the research presented. These two regulated DBPs can only be formed when bromide is present in the source water. However, UV technology is often used in conjunction with chlorination or other chemical disinfectants. The combination of chemical and photocatalytic oxidation may form THMs and HAAs. Analysis of the DOC concentration along with measuring THM and HAA formation before and after photocatalysis should provide a more complete understanding of the DBP formation potential associated with UV-TiO_2 photocatalysis.

6.3.3 Compare UV-NSTF with Other Immobilized TiO_2 Methods

Several methods of immobilizing various forms of TiO_2 are available in literature. To fully evaluate NSTF coated with TiO_2 by magnetron sputter deposition for oxidation, it should be directly compared to other methods, such as the sol-gel process. The suspected amorphous phase of TiO_2 present on the NSTF as a result of sputter deposition should be confirmed. The use of pCBA degradation as an indirect measure of •OH production is very useful, but actual disinfection trial should be completed to fully understand the synergy born from integrating UV technology and photoactive TiO_2. The production of Ct tables for various organisms would provide valuable information about how to

optimize TiO_2 photocatalysis for different applications, including drinking water and ballast water management. The Ct tables would also allow for direct comparison between this and other innovative, as well as conventional treatment methods.

Bibliography

Afkhami, A., T. Madrakian, and A. R. Zarei, 2001, Spectrophotometric determination of periodate, iodate and bromate mixtures based on their reaction with iodide: Analytical Sciences, v. 17, p. 1199-1202.

Agus, E., N. Voutchkov, and D. L. Sedlak, 2009, Disinfection by-products and their potential impact on the quality of water produced by desalination systems: A literature review: Desalination, v. 237, p. 214-237.

Auffan, M., J. Rose, M. Wiesner, and J. Bottero, 2009, Chemical stability of metallic nanoparticles: A parameter controlling their potential cellular toxicity in vitro: Environmental Pollution, p. 1127-1133.

Balasubramanian, G., D. D. Dionysiou, M. T. Suidan, Y. Subramanian, I. Baudin, and J. M. Laine, 2003, Titania powder modified sol-gel process for photocatalytic applications: Journal of Materials Science, v. 38, p. 823-831.

Berthouex, P. M., and L. C. Brown, 1994, Statistics for Environmental Engineers: Boca Raton, Lewis Publishers, 335 p.

Bolton, J., and K. Linden, 2003, Standardization of methods for fluence (UV dose) determination in bench-scale UV experiments: Journal of Environmental Engineering-ASCE, v. 129, p. 209-215.

Bonacquisti, T. P., 2006, A drinking water utility's perspective on bromide, bromate, and ozonation: Toxicology, v. 221, p. 145-148.

Bonakdarpour, A., T. R. Dahn, R. T. Atanasoski, M. K. Debe, and J. R. Dahn, 2008, H_2O_2 release during oxygen reduction reaction on Pt nanoparticles: Electrochemical and Solid State Letters, v. 11, p. B208-B211.

Bottero, J.-Y., J. Rose, and M. R. Wiesner, 2006, Nanotechnologies: tools for sustainability in a new wave of water treatment processes: Integr Environ Assess Manag, v. 2, p. 391-5.

Brunet, L., D. Y. Lyon, E. M. Hotze, P. J. J. Alvarez, and M. R. Wiesner, 2009, Comparative Photoactivity and Antibacterial Properties of C_{60} Fullerenes and Titanium Dioxoide Nanoparticles: Environmental Sci. Technology, v. 43, p. 4355-4360.

Butler, R., L. Lytton, A. Godley, I. Tothill, and E. Cartmell, 2005, Bromate analysis in groundwater and wastewater samples: Journal of Environmental Monitoring, v. 7, p. 999-1006.

Cabaj, A., R. Sommer, and D. Schoenen, 1996, Biodosimetry: Model calculations for UV water disinfection devices with regard to dose distributions: Water Research, v. 30, p. 1003-1009.

Cabrera, M. I., O. M. Alfano, and A. E. Cassano, 1996, Absorption and scattering coefficients of titanium dioxide particulate suspensions in water: Journal of Physical Chemistry, v. 100, p. 20043-20050.

Chen, Y. J., and D. D. Dionysiou, 2006, TiO_2 photocatalytic films on stainless steel: The role of Degussa P-25 in modified sol-gel methods: Applied Catalysis B-Environmental, v. 62, p. 255-264.

Chen, Y. J., and D. D. Dionysiou, 2008, Bimodal mesoporous TiO_2-P25 composite thick films with high photocatalytic activity and improved structural integrity: Applied Catalysis B-Environmental, v. 80, p. 147-155.

Cho, M., H. Chung, W. Choi, and J. Yoon, 2004, Linear correlation between inactivation of E-coli and OH radical concentration in TiO_2 photocatalytic disinfection: Water Research, v. 38, p. 1069-1077.

Cho, M., H. M. Chung, W. Y. Choi, and J. Y. Yoon, 2005, Different inactivation Behaviors of MS-2 phage and Escherichia coli in TiO2 photocatalytic disinfection: Applied and Environmental Microbiology, v. 71, p. 270-275.

Cho, M., and J. Yoon, 2008, Measurement of OH radical CT for inactivating Cryptosporidium parvum using photo/ferrioxalate and photo/TiO2 systems: Journal of Applied Microbiology, v. 104, p. 759-766.

Craik, S. A., D. W. Smith, M. S. Chandrakanth, and M. Belosevic, 2003, Efficient inactivation of Cryptosporidium parvum in a static mixer ozone contactor: Ozone-Science & Engineering, v. 25, p. 295-306.

Dahn, J. R., S. Trussler, T. D. Hatchard, A. Bonakdarpour, J. R. Mueller-Neuhaus, K. C. Hewitt, and M. Fleischauer, 2002, Economical sputtering system to produce large-size composition-spread libraries having linear and orthogonal stoichiometry variations: Chemistry of Materials, v. 14, p. 3519-3523.

Debe, M. K., 2003, Novel catalysts, catalyst support and catalysts coated membrane methods, *in* W. Vielstich, H. A. Gasteiger, and A. Lamm, eds., Handbook of Fuel

Cells - Fundamentals, Technology and Applications, v. 3, John Wiley & Sons, Ltd.

Debe, M. K., and A. R. Drube, 1995, Structural characteristics of a uniquely nanostructured organic thin-film: Journal of Vacuum Science & Technology B, v. 13, p. 1236-1241.

Debe, M. K., and R. J. Poirier, 1994, Postdeposition growth of a uniquely nanostructured organic film by vacuum annealing: Journal of Vacuum Science & Technology a-Vacuum Surfaces and Films, v. 12, p. 2017-2022.

Debe, M. K., A. K. Schmoeckel, G. D. Vernstrorn, and R. Atanasoski, 2006, High voltage stability of nanostructured thin film catalysts for PEM fuel cells: Journal of Power Sources, v. 161, p. 1002-1011.

Dobroski, N., C. Scianni, D. Gehringer, and M. Falkner, 2009, 2009 Assessment of the Efficacy, Availability and Environmental Impacts of Ballast Water Treatment Systems for Use in California Waters, California State Lands Commission, Marine Facilities Division.

Elovitz, M. S., and U. von Gunten, 1999, Hydroxyl radical ozone ratios during ozonation processes. I - The R_{ct} concept: Ozone-Science & Engineering, v. 21, p. 239-260.

Ensafi, A. A., and G. B. Dehaghi, 2000, Flow-injection simultaneous determination of iodate and periodate by spectrophotometric and spectrofluorometric detection: Analytical Sciences, v. 16, p. 61-64.

Erdem, B., R. A. Hunsicker, G. W. Simmons, E. D. Sudol, V. L. Dimonie, and M. S. El-Aasser, 2001, XPS and FTIR surface characterization of TiO_2 particles used in polymer encapsulation: Langmuir, v. 17, p. 2664-2669.

Fitzmaurice, D. J., M. Eschle, H. Frei, and J. Moser, 1993, Time-resolved rise of I_2^- upon oxidation of iodide at aqueous TiO_2 colloid: Journal of Physical Chemistry, v. 97, p. 3806-3812.

Fukushi, K., R. Yamazaki, and T. Yamane, 2009, Determination of bromate in highly saline samples using CZE with on-line transient ITP: Journal of Separation Science, v. 32, p. 457-461.

Gancs, L., T. Kobayashi, M. K. Debe, R. Atanasoski, and A. Wieckowski, 2008, Crystallographic characteristics of nanostructured thin-film fuel cell electrocatalysts: A HRTEM study: Chemistry of Materials, v. 20, p. 2444-2454.

Gerischer, H., 1993, Conditions for an efficient photocatalytic activity of TiO_2 particles, *in* D. F. Ollis, and H. Alekabi, eds., Photocatalytic Purification and Treatment of Water and Air: Trace Metals in the Environment, v. 3: Amsterdam, Elsevier Science Publ B V, p. 1-17.

Gerrity, D., H. Ryu, J. Crittenden, and M. Abbaszadegan, 2008, Photocatalytic inactivation of viruses using titanium dioxide nanoparticles and low-pressure UV light: Journal of Environmental Science and Health, Part A, v. 43, p. 1261 - 1270.

Gilpin Jr., E., and C. S. o. C. Engineers, 2009, The Iron Ores of Nova Scotia, BiblioBazaar, LLC, 32 p.

Gopel, W., G. Rocker, and R. Feierabend, 1983, Intrinsic defects of TiO_2(110): Interaction with chemisorbed O_2, H_2, CO, and CO_2: Physical Review B, v. 28, p. 3427-3438.

Gregg, M., G. Rigby, and G. M. Hallegraeff, 2009, Review of two decades of progress in the development of management options for reducing or eradicating phytoplankton, zooplankton and bacteria in ship's ballast water: Aquatic Invasions, v. 4, p. 521-565.

Hand, D. W., D. L. Perram, and J. C. Crittenden, 1995, Destruction of DBP precursors with catalytic oxidation: American Water Works Association Journal, v. 87, p. 84-96.

Hartmann, N. B., F. Von der Kammer, T. Hofmann, M. Baalousha, S. Ottofuelling, and A. Baun, 2010, Algal testing of titanium dioxide nanoparticles-Testing considerations, inhibitory effects and modification of cadmium bioavailability: Toxicology, v. 269, p. 190-197.

Henglein, A., 1982, Colloidal TiO_2 catalyzed photo- and radiation chemical processes in aqueous solution: Berichte Der Bunsen-Gesellschaft-Physical Chemistry Chemical Physics, v. 86, p. 241-246.

Hofmann, R., and R. C. Andrews, 2001, Ammoniacal bromamines: A review of their influence on bromate formation during ozonation: Water Research, v. 35, p. 599-604.

International Maritime Organization, 2009, International Convention for the Control and Management of Ships' Ballast Water and Sediments adopted in 2004.

Jones, A. C., R. W. Gensemer, W. A. Stubblefield, E. Van Genderen, G. M. Dethloff, and W. J. Cooper, 2006, Toxicity of ozonated seawater to marine organisms: Environmental Toxicology and Chemistry, v. 25, p. 2683-2691.

Kim, J. H., M. S. Elovitz, U. von Gunten, H. M. Shukairy, and B. J. Marinas, 2007, Modeling Cryptosporidium parvum oocyst inactivation and bromate in a flow-through ozone contactor treating natural water: Water Research, v. 41, p. 467-475.

Koivunen, J., and H. Heinonen-Tanski, 2005, Inactivation of enteric microorganisms with chemical disinfectants, UV irradiation and combined chemical/UV treatments: Water Research, v. 39, p. 1519-1526.

Kuo, J., C. L. Chen, and M. Nellor, 2003, Standardized collimated beam testing protocol for water/wastewater ultraviolet disinfection: Journal of Environmental Engineering-Asce, v. 129, p. 774-779.

Kwon, S., M. Fan, A. T. Cooper, and H. Q. Yang, 2008, Photocatalytic applications of micro- and Nano-TiO_2 in environmental engineering: Critical Reviews in Environmental Science and Technology, v. 38, p. 197-226.

Legube, B., 1996, A survey of bromate ion in European drinking water: Ozone-Science & Engineering, v. 18, p. 325-348.

Linsebigler, A. L., G. Q. Lu, and J. T. Yates, 1995, Photocatalysis on TiO_2 surfaces: Principles, mechanisms, and selected results: Chemical Reviews, v. 95, p. 735-758.

Liu, G. C. K., R. J. Sanderson, G. Vernstrom, D. A. Stevens, R. T. Atanasoski, M. K. Debe, and J. R. Dahn, 2010, RDE Measurements of ORR Activity of $Pt_{1-x}Ir_x$ ($0 < x < 0.3$) on High Surface Area NSTF-Coated Glassy Carbon Disks: Journal of the Electrochemical Society, v. 157, p. B207-B214.

Liu, S., M. Lim, R. Fabris, C. Chow, M. Drikas, and R. Amal, 2008, TiO_2 photocatalysis of natural organic matter in surface water: Impact on trihalomethane and haloacetic acid formation potential: Environmental Science & Technology, v. 42, p. 6218-6223.

Malley, J. P., J. R. Shaw, and J. R. Ropp, 1996, Evaluation of by-products produced by treatment of groundwaters with ultraviolet irradiation: Denver, The Foundation and American Water Works Association, 115 p.

Matilainen, A., and M. Sillanpaa, 2010, Removal of natural organic matter from drinking water by advanced oxidation processes: Chemosphere, v. 80, p. 351-365.

Moser, J., and M. Gratzel, 1982, Photoelectrochemistry with colloidal semiconductors: Laser studies of halide oxidation in colloidal dispersions of TiO_2 and alpha-Fe_2O_3: Helvetica Chimica Acta, v. 65, p. 1436-1444.

Neta, P., and L. M. Dorfman, 1968, Pulse radiolysis studies. XIII: Rate constants for reaction of hydroxyl radicals with aromatic compounds in aqueous solutions.: Advances in Chemistry Series, p. 222-&.

Peller, J. R., R. L. Whitman, S. Griffith, P. Harris, C. Peller, and J. Scalzitti, 2007, TiO_2 as a photocatalyst for control of the aquatic invasive alga, Cladophora, under natural and artificial light: Journal of Photochemistry and Photobiology a-Chemistry, v. 186, p. 212-217.

Pereira, V. J., H. S. Weinberg, K. G. Linden, and P. C. Singer, 2007, UV degradation kinetics and modeling of pharmaceutical compounds in laboratory grade and surface water via direct and indirect photolysis at 254 nm: Environmental Science & Technology, v. 41, p. 1682-1688.

Perrins, J. C., W. J. Cooper, J. H. van Leeuwen, and R. P. Herwig, 2006, Ozonation of seawater from different locations: Formation and decay of total residual oxidant - implications for ballast water treatment: Marine Pollution Bulletin, v. 52, p. 1023-1033.

Pi, Y. Z., J. Schumacher, and M. Jekel, 2005, The use of para-chlorobenzoic acid (pCBA) as an ozone/hydroxyl radical probe compound: Ozone-Science & Engineering, v. 27, p. 431-436.

Rennecker, J. L., B. J. Marinas, J. H. Owens, and E. W. Rice, 1999, Inactivation of Cryptosporidium parvum oocysts with ozone: Water Research, v. 33, p. 2481-2488.

Rosenfeldt, E. J., and K. G. Linden, 2007, The $R_{OH,UV}$ concept to characterize and the model UV/H_2O_2 process in natural waters: Environmental Science & Technology, v. 41, p. 2548-2553.

Ryu, H., D. Gerrity, J. C. Crittenden, and M. Abbaszadegan, 2008, Photocatalytic inactivation of Cryptosporidium parvum with TiO_2 and low-pressure ultraviolet irradiation: Water Research, v. 42, p. 1523-1530.

Sanches, S., M. T. B. Crespo, and V. J. Pereira, 2010, Drinking water treatment of priority pesticides using low pressure UV photolysis and advanced oxidation processes: Water Research, v. 44, p. 1809-1818.

Shultz, A. N., W. Jang, W. M. Hetherington, D. R. Baer, L. Q. Wang, and M. H. Engelhard, 1995, Comparative 2nd-harmonic generation and x-ray photoelectron-spectroscopy studies of the UV creation and O_2 healing of Ti^{3+} defects on (110) rutile TiO_2 surfaces: Surface Science, v. 339, p. 114-124.

Singer, P. C., 2006, DBPs in drinking water: Additional scientific and policy considerations for public health protection: Journal American Water Works Association, v. 98, p. 73-+.

Song, R. G., C. Donohoe, R. Minear, P. Westerhoff, K. Ozekin, and G. Amy, 1996, Empirical modeling of bromate formation during ozonation of bromide-containing waters: Water Research, v. 30, p. 1161-1168.

Song, W., V. Ravindran, B. E. Koel, and M. Pirbazari, 2004, Nanofiltration of natural organic matter with H_2O_2/UV pretreatment: fouling mitigation and membrane surface characterization: Journal of Membrane Science, v. 241, p. 143-160.

Tango, M., and G. Gagnon, 2003, Impact of ozonation on water quality in marine recirculation systems: Aquacultural Engineering, v. 29, p. 125-137.

Tercero Espinoza, L. A., and F. H. Frimmel, 2008, Formation of brominated products in irradiated titanium dioxide suspension containing bromide and dissolved organic carbon: Water Research, v. 42, p. 1778-1784.

Thiruvenkatachari, R., S. Vigneswaran, and I. S. Moon, 2008, A review on UV/TiO_2 photocatalytic oxidation process: Korean Journal of Chemical Engineering, v. 25, p. 64-72.

USEPA, 1999, Method 300.1 - Determination of Inorganic Anions in Drinking Water by Ion Chromatography. Revision 1.0, *in* USEPA, ed., Cincinnati.

USEPA, 2000, U.S. EPA Volatile Organics Method 524.2 Using Purge and Trap GC/MS, *in* USEPA, ed.

USEPA, 2006, Ultraviolet Disinfection Guidance Manual for the Final Long Term 2 Enhanced Surface Water Treatment Rule, Washington, D.C., USEPA, p. 1-436.

USEPA, 2009, Drinking Water Contaminants.

von Gunten, U., 2003a, Ozonation of drinking water: Part I. Oxidation kinetics and product formation: Water Research, v. 37, p. 1443-1467.

von Gunten, U., 2003b, Ozonation of drinking water: Part II. Disinfection and by-product formation in presence of bromide, iodide or chlorine: Water Research, v. 37, p. 1469-1487.

von Gunten, U., and J. Hoigne, 1994, Bromate formation during ozonation of bromide-containing waters - Interaction of ozone and hydroxyl radical reactions: Environmental Science & Technology, v. 28, p. 1234-1242.

Wang, L. Q., D. R. Baer, and M. H. Engelhard, 1995, The adsorption of liquid and vapor water on TiO_2 (110) surfaces: The role of defects: Structure and Properties of Interfaces in Ceramics, v. 357, p. 97-102.

Wang, R., N. Sakai, A. Fujishima, T. Watanabe, and K. Hashimoto, 1999, Studies of surface wettability conversion on TiO_2 single-crystal surfaces: Journal of Physical Chemistry B, v. 103, p. 2188-2194.

Watts, M. J., and K. G. Linden, 2007, Chlorine photolysis and subsequent OH radical production during UV treatment of chlorinated water: Water Research, v. 41, p. 2871-2878.

Watts, M. J., E. J. Rosenfeldt, and K. G. Linden, 2007, Comparative OH radical oxidation using UV-Cl_2 and UV-H_2O_2 processes: Journal of Water Supply Research and Technology-Aqua, v. 56, p. 469-477.

Westerhoff, P., R. Song, G. Amy, and R. Minear, 1998, Numerical kinetic models for bromide oxidation to bromine and bromate: Water Research, v. 32, p. 1687-1699.

Yao, C. C. D., and W. R. Haag, 1991, Rate constants for direct reactions of ozone with several drinking-water contaminants: Water Research, v. 25, p. 761-773.

Yu, J. G., X. J. Zhao, J. C. Du, and W. M. Chen, 2000, Preparation, microstructure and photocatalytic activity of the porous TiO_2 anatase coating by sol-gel processing: Journal of Sol-Gel Science and Technology, v. 17, p. 163-171.

Appendix A – Bromate Detection Method Data

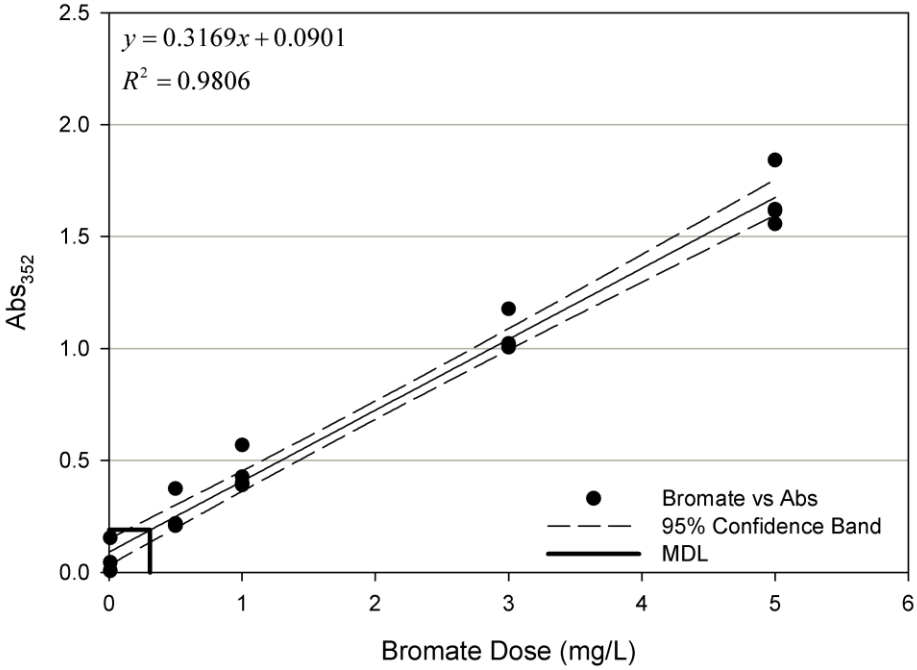

Figure 25. Bromate concentration in tap water (Halifax Regional Municipality) is calculated based on the observed absorbance.

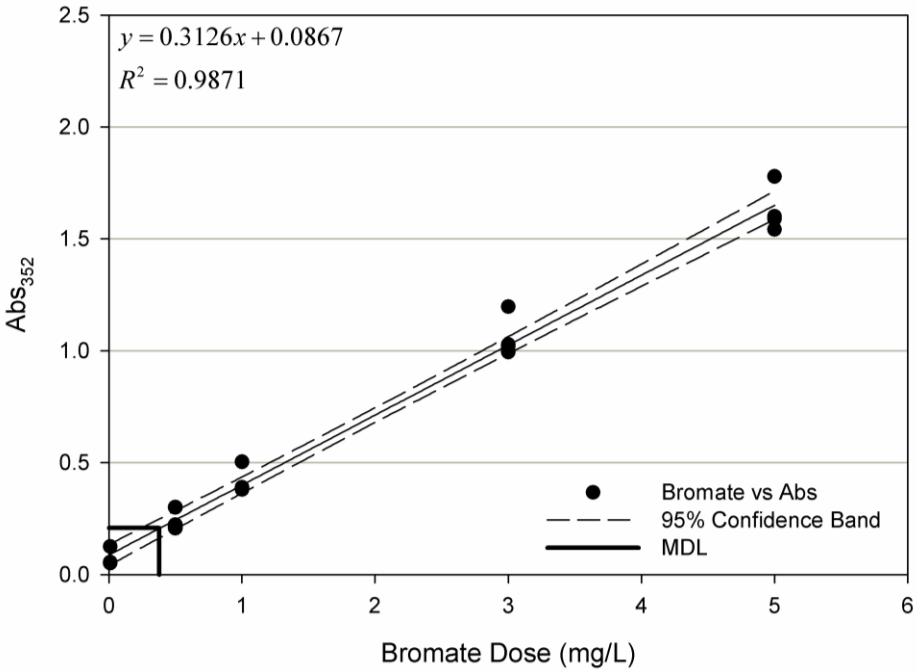

Figure 26. Bromate concentration in dechlorinated tap water from Halifax Regional Municipality is calculated based on the observed absorbance.

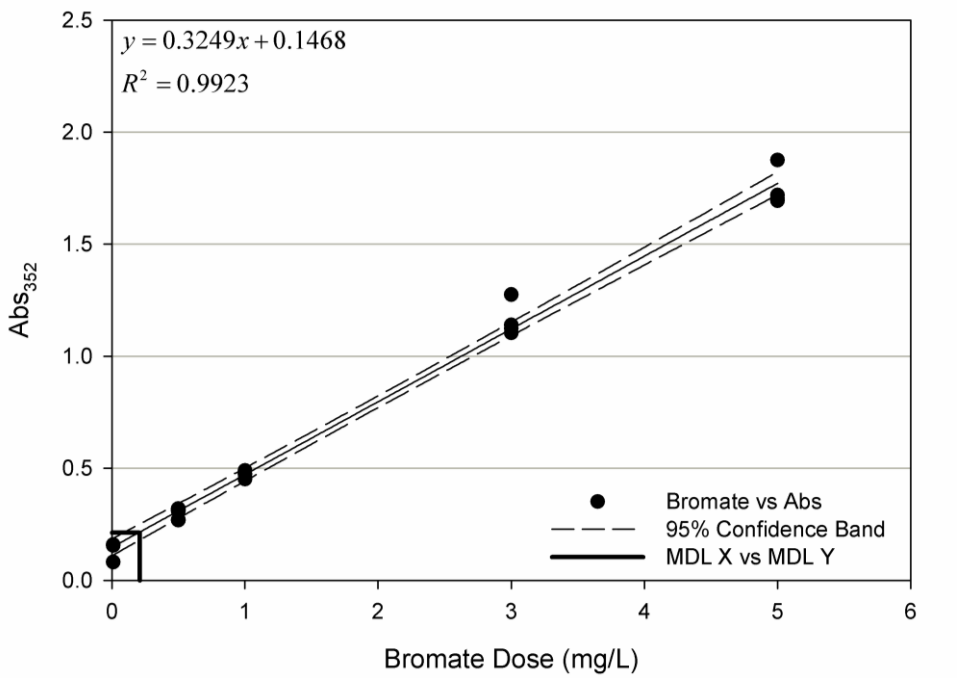

Figure 27. Bromate concentration in Tatamagouche (French River) raw water is calculated based on the observed absorbance.

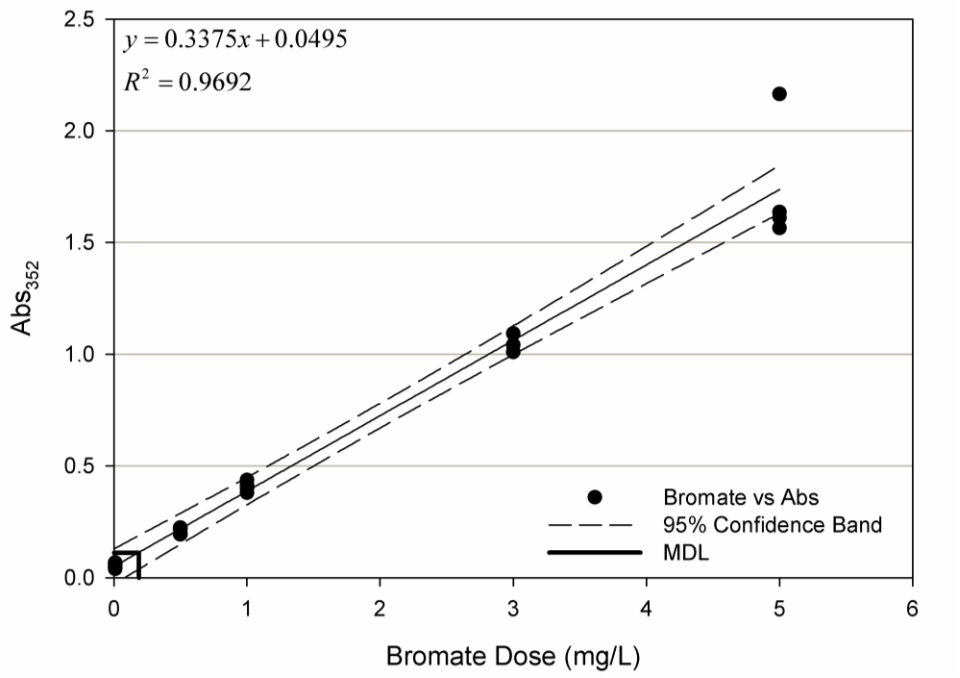

Figure 28. Bromate concentration in Shelburne (Rodney Lake) raw water is calculated based on the observed absorbance.

Figure 29. Bromate dose vs. measured bromate by ion chromatography in Milli-Q water.

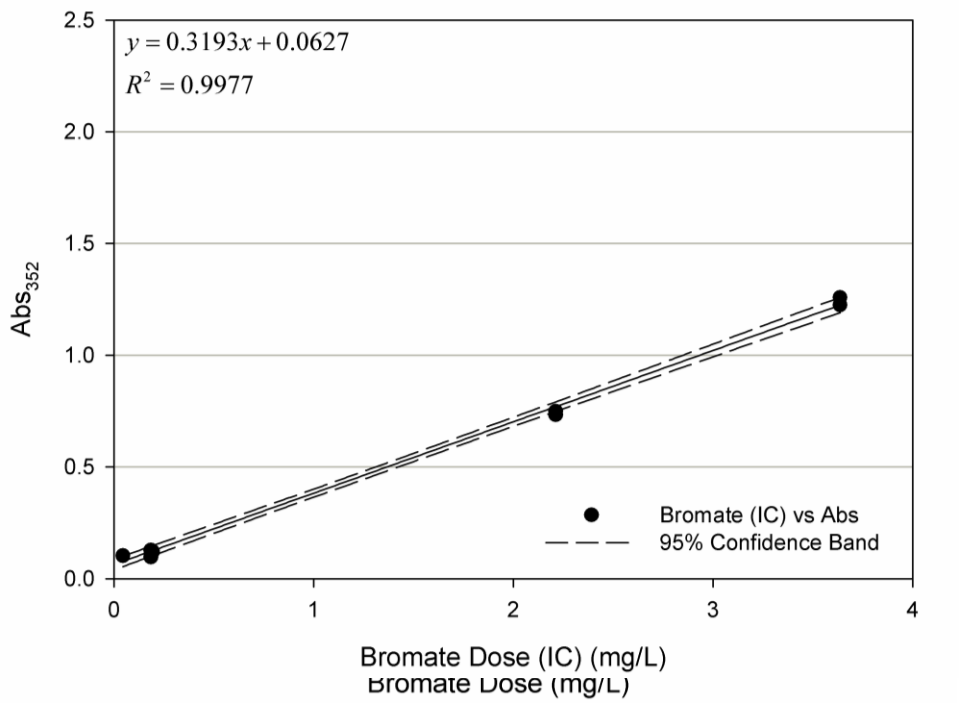

Figure 30. Measured bromate by ion chromatography in Milli-Q water vs. UV absorbance at 352 nm.

Appendix B – XPS Comparison Data of TiO_2 on NSTF

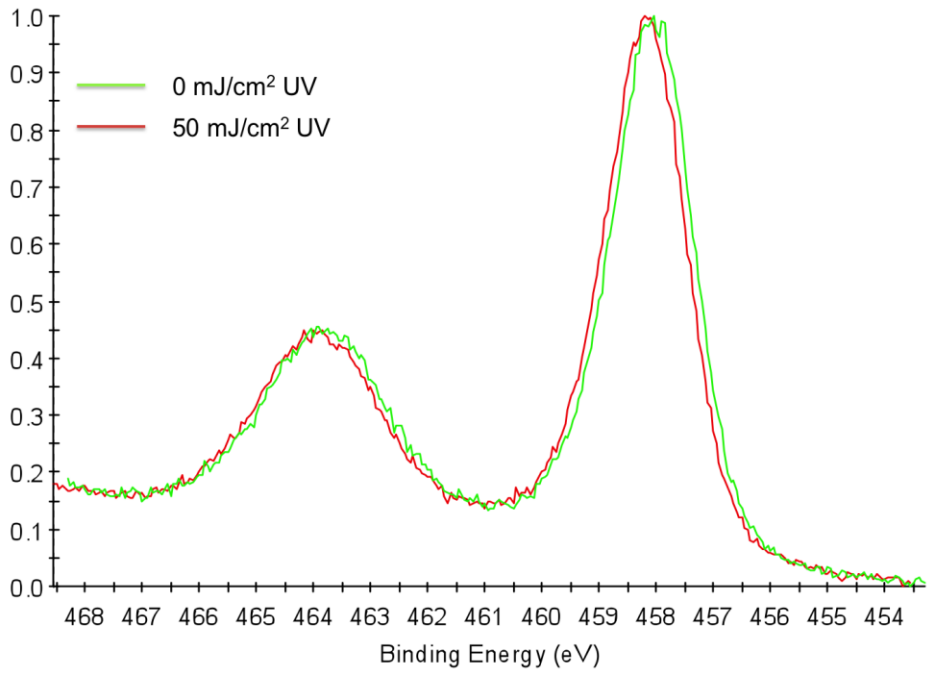

Figure 31. High-resolution XPS spectra comparison of the Ti2p peak as deposited on NSTF before and after 50 mJ/cm^2 UV irradiation in Milli-Q water.

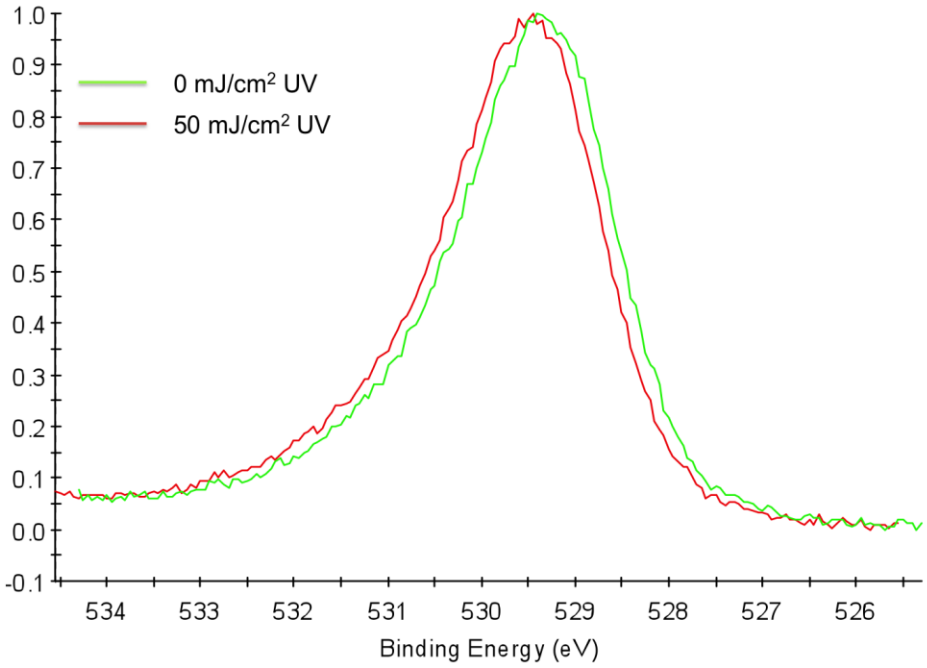

Figure 32. High-resolution XPS spectra comparison of the O1s peak as deposited on NSTF before and after 50 mJ/cm^2 UV irradiation in Milli-Q water.

Appendix C – k^* Calculation Data

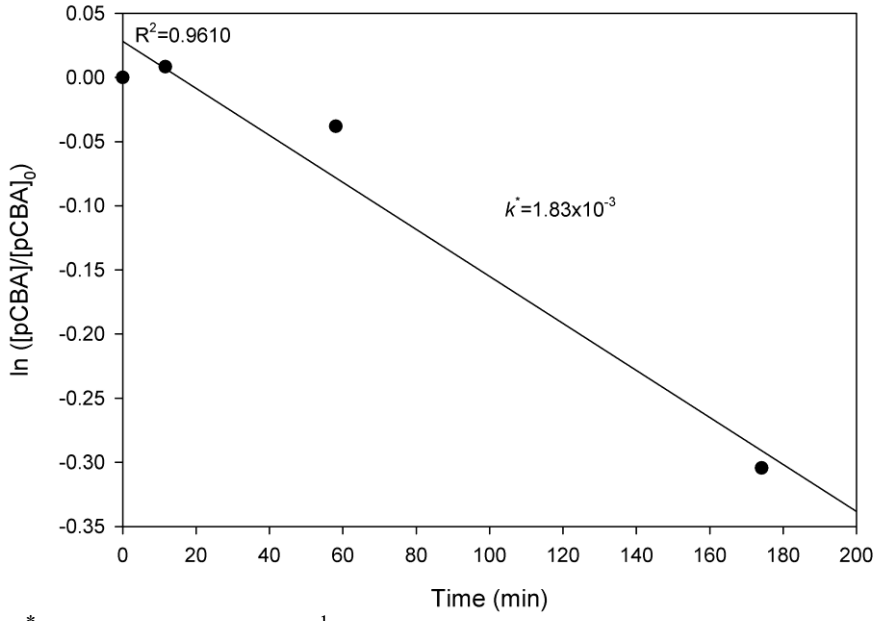

Figure 33. k^* calculation of 1 mgL^{-1} TiO_2 supported on NSTF.

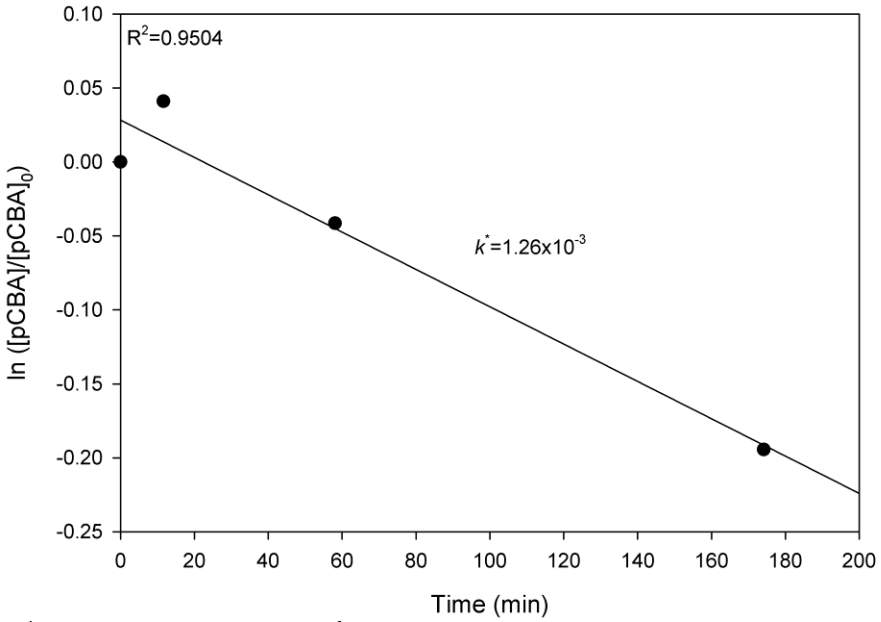

Figure 34. k^* calculation of 10 mgL^{-1} TiO_2 supported on NSTF.

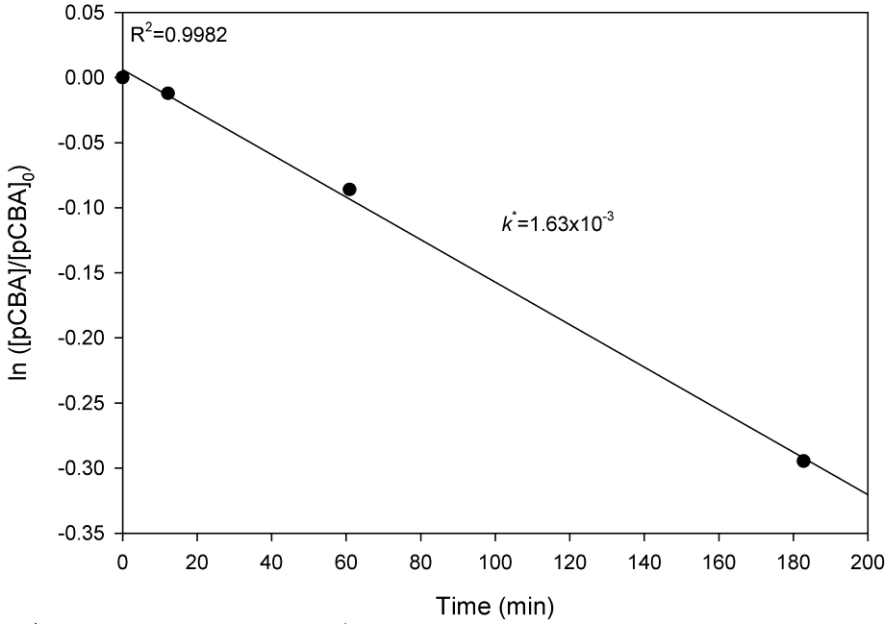

Figure 35. k^* calculation of 10 mgL^{-1} suspended TiO_2 nanoparticles.

Appendix D – NSTF Stability After UV Irradiation Data

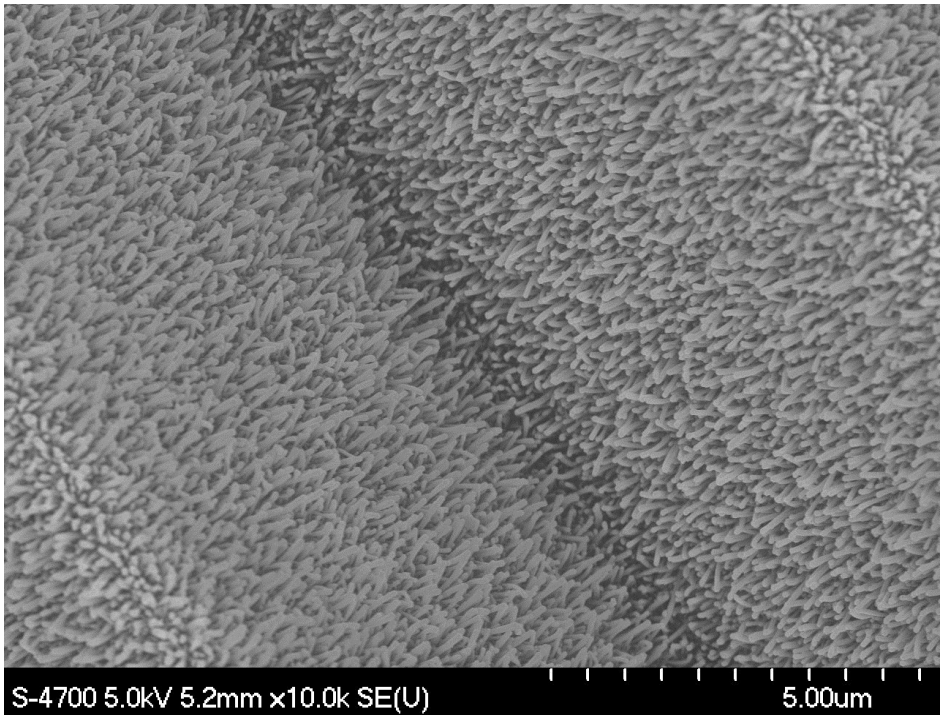

Figure 36. NSTF coated with 300 nm (planar equivalent) TiO_2 after irradiation of 50 mJ/cm2 UV light in Milli-Q water. No changes are observed after irradiation.

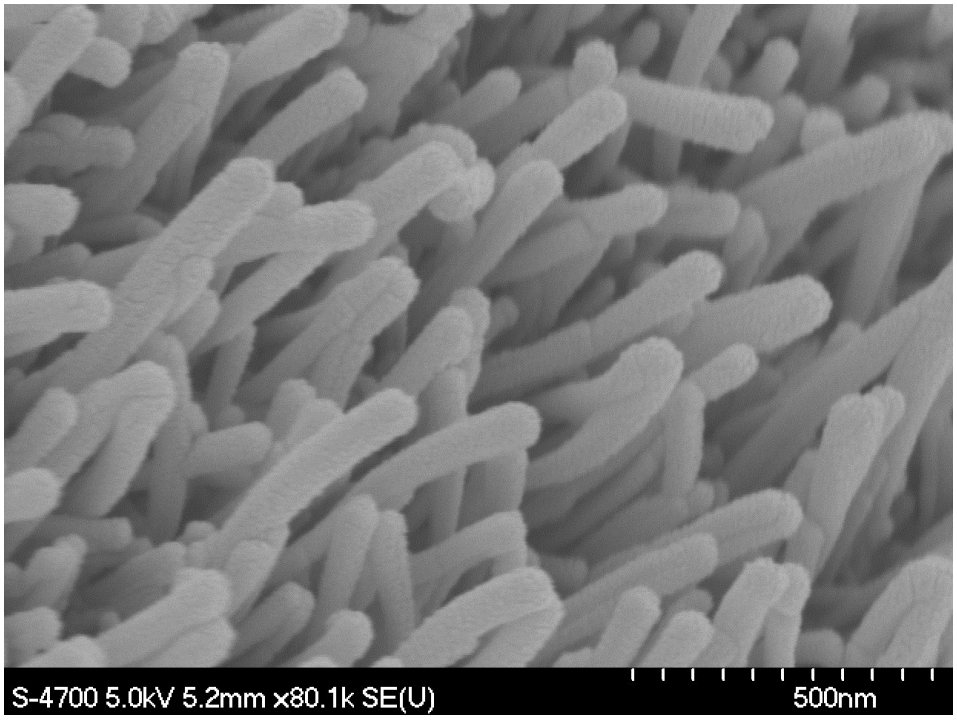

Figure 37. NSTF coated with 300 nm (planar equivalent) TiO_2 after irradiation of 50 mJ/cm2 UV light in Milli-Q water. No changes are observed after irradiation.